



## **CHAPTER 2**

**SYNTHESIS  
AND  
CHARACTERIZATION  
OF  
M(IV) PHOSPHATES  
M(IV) TUNGSTATES  
RUTHENIUM EXCHANGED PHASES  
OF  
M(IV) PHOSPHATES AND  
TUNGSTATES**

## 2.1 INTRODUCTION

The successful operation of catalytic processes depends on the properties of the catalyst itself. These properties are function of the method of synthesis adopted. The challenge for the chemist, by the demands of catalytic processes, is to design and synthesize in high yield, novel catalysts, whose structures and properties can be predicted, varied and controlled, through eco-friendly routes. Catalyst preparation is continuously becoming more imaginative and dependent on a multidisciplinary approach. The interest in novel catalysts with predictable structures and properties for specific applications has given rise to the development of a variety of preparation methodologies. Some of the synthetic procedures available to the inorganic chemist for the preparation of bulk solids are –

- 1 Coprecipitation
- 2 Hydrothermal methods
- 3 Electrochemical methods
- 4 Vapor phase transport
- 5 High pressure synthesis
- 6 Pyrolysis
- 7 Photolysis
- 8 Intercalation
- 9 Sol-gel processes
- 10 Ion exchange

With an increasing concern around the world for green technologies, much attention is focused towards the development of alternative synthetic routes which have zero emission. From an industrial point of view, a method that does not employ high temperatures, could be favoured, because of the ensuing energy savings.

Growing and stringent environmental regulations world wide, demand , making use of soft chemistry routes (low temperatures) which is popularly known as “Chemie Douce” by the French. Soft chemistry routes include, sol-gel method of synthesis, ion exchange, intercalation, hydrolysis, dehydration and reduction, that can be carried out at relatively low temperatures.

The traditional ceramic method consists of heating together two solids, with intermittent mixing and grinding, which react to form the required product. Despite the widespread use in industries as well as in the laboratories, it has certain disadvantages; high synthesis temperatures, which require large energy inputs and the reactions are slow, since they are generally carried out in the solid state. Besides, the homogeneity of the reactants, is a big issue to be taken care of, for the phasic purity of the desired product.

The present chapter deals with the synthesis and characterization of the following materials

1. AMORPHOUS MATERIALS

Zirconium phosphate (ZrP)

Titanium phosphate (TiP)

Tin phosphate (SnP)

Zirconium tungstate (ZrW)

Titanium tungstate (TiP)

Tin tungstate (SnW)

2. CRYSTALLINE MATERIALS

Zirconium phosphate (ZrPcry)

Titanium phosphate (TiPcry)

Tin phosphate (SnPcry)

3. METAL EXCHANGED PHASES

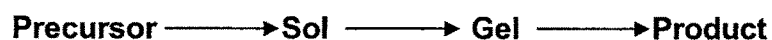
Ru(III) exchanged – Ru(III)ZrP, Ru(III)TiP, Ru(III)SnP, Ru(III)ZrW, Ru(III)TiW, Ru(III)SnW

Ru exchanged – RuZrP, RuTiP, RuSnP, RuZrW, RuTiW, RuSnW

Amorphous M(IV) phosphates have been prepared by sol-gel technique, crystalline M(IV) phosphates have been prepared by the reflux method [1] and metal exchanged phases have been prepared by ion exchange technique.

**2.2 SOL-GEL PROCESS**

The overall sol-gel process can be represented by the following sequence of transformations:



**Precursors** are starting materials, in which the essential basic entities for further network formation are present in the correct stoichiometry.

**Sol** is a colloidal suspension of particles in a liquid, the particles typically ranging from 1–100 nm in diameter.

**Gel** is a semi-rigid solid, in which solvent is contained in a framework of material, which is either colloidal (essentially a concentrated sol) or polymeric.

Sol-gel process can be distinguished from precipitation by its specific property to stabilize a finely dispersed (mostly colloidal) phase in solution by surface chemistry. The size of solid agglomerates is usually in the range 1-100 nm.

Important steps involved in sol-gel synthesis are –

**Hydrolysis** – It involves reaction of inorganic or organometallic precursor with water or a solvent, at ambient or slightly elevated temperature. Acid or base catalysts are added to speed up the reaction.

**Polymerization** – This step involves condensation of adjacent molecules wherein H<sub>2</sub>O and alcohol are eliminated and metal oxide linkages are formed. Polymeric networks grow to colloidal dimensions in the liquid (sol) state.

**Gelation** – It leads to the formation of a three dimensional network throughout the liquid, by the linking up of polymeric networks. The system becomes somewhat rigid, characteristic of a gel, on removing the solvent from the sol. Aggregation of the small polymeric units, to the main network structure progressively continues on ageing the gel.

**Drying** – Here solvent is removed at moderate temperatures (< 470 K) leaving the residue behind. For obtaining high surface area and low bulk density aerogel powders, the solvent is removed supercritically.

**Dehydration** – This step is carried out between 670 and 1070 K to drive off the organic residues and chemically bound water, yielding a glassy metal oxide with up to 20–30% microporosity.

**Densification** – Temperature in excess of 1270 K are used to form the dense oxide product.

The choice of reagents, additives, concentration, ionic strength of reactants, pH, addition sequence, reaction and drying conditions, allows the control of pore structure and porosity, composition, surface polarity, surface acidity and crystallinity.

In practice however, a modified sol-gel route is followed. One of the important features in this modified route is the use of templates (structure directing agents). Templates when used at optimum concentrations, referred to as Critical Micelle Concentration (CMC), orient themselves to form an assembly with the polar head groups pointing outside, around which the anions orient to form a network. The layers of inorganic materials seem to distort and crosslink around the polar head groups to form a new mesoporous structure. The driving force for this layer folding, is most likely the ion pairing between the positively charged ammonium head groups and the negatively charged inorganic components. The template can subsequently be removed from the system, either by solvent extraction method or by calcination, to obtain finished product with predetermined pore size and structure. The sol gel method presents an attractive and easy-to-tailor alternative to conventional synthesis methods, such as ceramic firing.

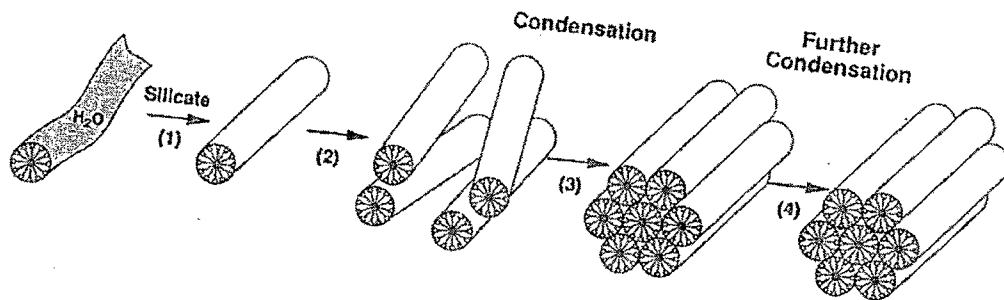


Figure 1. Mechanism of template assisted synthesis reproduced from [2].

### Advantages of Sol-Gel Process

1. High homogeneity - intimate mixing of raw materials
2. High purity
3. Low temperature processing
  - a. energy savings
  - b. minimize evaporation losses
  - c. minimize air pollution
  - d. no reaction with container
4. More uniform phase distribution in multicomponent systems
5. New crystalline phases from new noncrystalline solids
6. Better glass products from special properties of gel

7. Materials with improved and desired properties (Tailor made materials) can be obtained
8. Porous materials using templates

#### **Disadvantages of the Sol-Gel Process**

1. Large shrinkage during processing
2. Residual fine pores
3. Residual hydroxyl groups when hydroxides are used
4. Residual carbon (originating from templates)
5. Health hazards of organic solvents
6. Long processing times

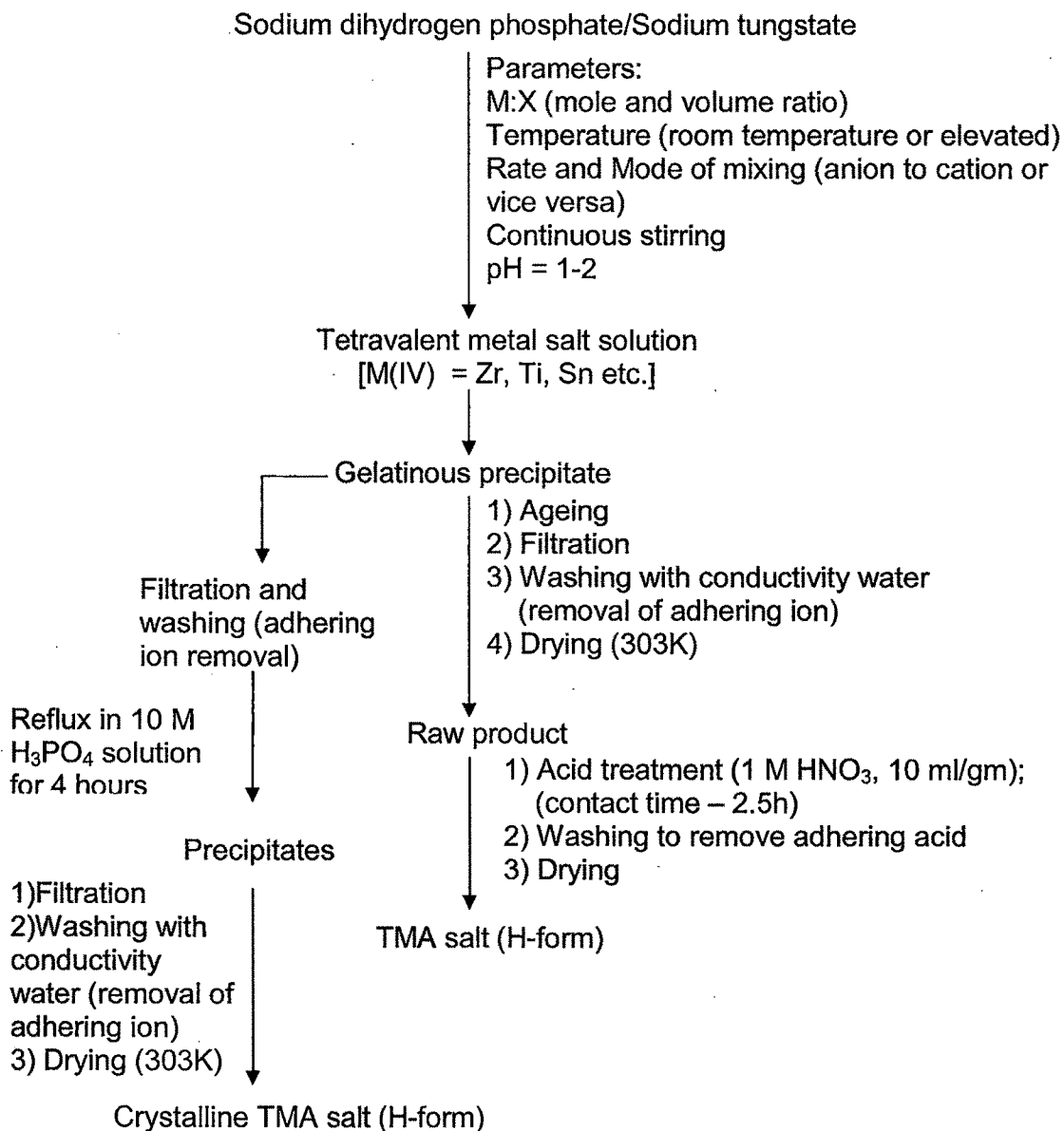
#### **2.3 ION EXCHANGE**

Ion-exchange is defined as a process, where an insoluble substance removes ions of positive or negative charge, from an electrolyte solution and releases other ions of like charge into solution, in a chemically equivalent amount. At some point, during the ion exchange process, ion exchange equilibrium is established. Ion exchange is, with few exceptions, a reversible process.

Of late, one of the growing applications of ion exchange has been in the area of Heterogenised Homogeneous Catalysis. Homogeneous catalysts are heterogenised by supporting them onto insoluble supports, in such a manner that the environment of the catalyst is essentially unchanged. The term heterogenising refers to a process, whereby a homogeneous transition metal ion or a metal complex is immobilized or anchored onto an inert support. The supports mainly used so far are organic polymeric supports (ion exchange resins) and the inorganic oxides – silica, alumina, zirconia etc. Though the method of anchoring on organic resins is a simple ion exchange technique, the greatest drawback is poor heat transfer ability which leads to degradation at low temperatures. On the other hand, inorganic oxides though thermally stable upto fairly high temperatures do not possess proper sites for anchoring (only weak hydroxyl groups are present on the surface). The ideal material to be used as support is therefore the tma salts. Due to cation exchange properties, the method of anchoring is simple. Besides, the material also possesses good thermal stability.

## 2.4 SYNTHETIC ROUTE FOR SYNTHESIS OF M(IV) PHOSPHATES AND TUNGSTATES:

A general procedure is presented in the following scheme



## 2.5 EXPERIMENTAL

### Materials

Zirconium oxychloride ( $\text{ZrOCl}_2 \cdot 8\text{H}_2\text{O}$ ), Titanium tetrachloride ( $\text{TiCl}_4$ ) and Stannic tetrachloride ( $\text{SnCl}_4$ ) were procured from Loba chemicals. Sodium dihydrogen phosphate ( $\text{NaH}_2\text{PO}_4 \cdot 2\text{H}_2\text{O}$ ), Sodium tungstate ( $\text{Na}_2\text{WO}_4 \cdot 2\text{H}_2\text{O}$ ) and  $\text{H}_3\text{PO}_4$  were obtained from Merck India. Ruthenium chloride was procured from Loba chemicals.  $\text{H}_2\text{SO}_4$ ,  $\text{HNO}_3$ ,  $\text{HCl}$ ,  $\text{NaOH}$ ,  $\text{KOH}$  and organic solvents used were of analytical grade.

### Synthesis of M(IV) phosphates and tungstates

M (IV) phosphates and tungstates were prepared by sol-gel method. Aqueous solution (0.2 M, 100 mL) of sodium dihydrogen phosphate or sodium tungstate was added drop wise to an aqueous solution (0.1 M, 100 mL) of zirconium oxy chloride or titanium tetrachloride (20%  $\text{HCl}$ ) or stannic tetrachloride with continuous stirring for 2h, maintaining the resultant solution temperature at  $70^\circ\text{C}$  and  $\text{pH} \sim 2$ . A gel was formed and the solution along with the gel was further stirred for an hour. The gel was filtered, washed with conductivity water till free of chloride ions (step 1) and dried at room temperature.

All the materials were converted to acid form by treating 5 g of the material with 50 mL of 1M  $\text{HNO}_3$  for 30 min. with occasional shaking. The sample was then separated from acid by decantation and washed with conductivity water for removal of adhering acid. This process (acid treatment) was repeated at least five times. After final washing, the material was dried at room temperature. This material was used for all studies.

In order to synthesize crystalline material, the gel obtained in (step 1) was refluxed in 10 M  $\text{H}_3\text{PO}_4$  solution for 4 hours and then filtered, washed to remove adhering ions and dried at  $373^\circ\text{K}$ .

### Synthesis of metal exchanged phases

#### *Synthesis of Ru(III)ZrP, Ru(III)TiP, Ru(III)SnP, Ru(III)ZrW, Ru(III)TiW and Ru(III)SnW*

Ru(III) exchanged phases have been prepared by equilibrating aqueous  $\text{RuCl}_3$  solution (0.1% w/v, 100 ml) with 2 g ZrP, TiP, SnP, ZrW, TiW, SnW as the case may be, with continuous stirring at 323 K for 48 h. The solid was

separated by filtration and washed with conductivity water for removal of adhering ions and dried at room temperature.

***Synthesis of RuZrP, RuTiP, RuSnP, RuZrW, RuTiW and RuSnW***

Ru(III) supported onto M(IV) phosphates and tungstates was reduced to Ru by treating with hydrogen in a 500 ml autoclave at 200 °C for 1 hr to give RuZrP, RuTiP, RuSnP and RuZrW, RuTiW and RuSnW. Temperature programmed reduction technique was used to determine reduction temperature of Ru(III) to Ru(0). In order to determine the reduction temperature of Ru(III) to Ru(0), temperature programmed reduction of supported catalyst was carried out on Micromeritics Chemisorb 2720 using 10 % H<sub>2</sub>+N<sub>2</sub> up to 700 °C. Figure 2 indicates reduction temperature of Ru(III) at 190 °C and beyond this temperature no peak is observed indicating that all Ru(III) sites are reduced to Ru(0).

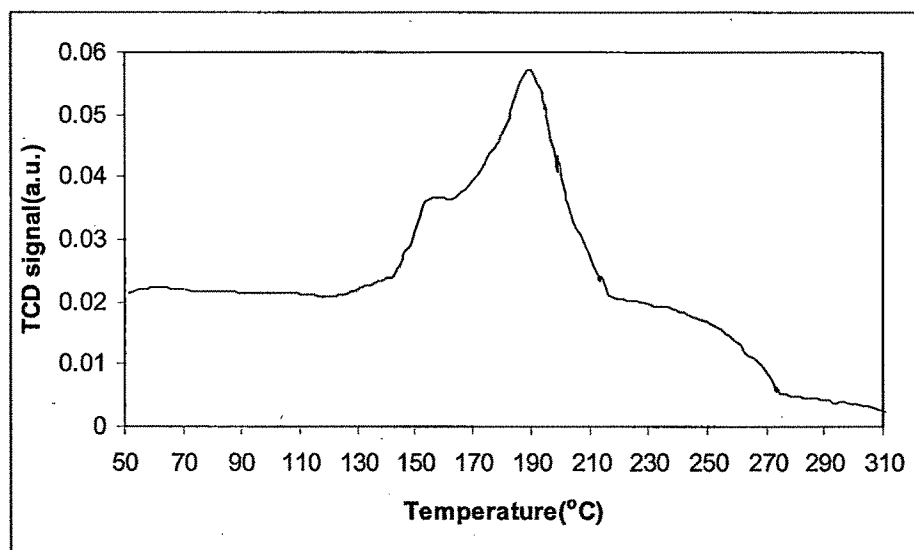


*Figure 2. TPR pattern of Ru(III)ZrP*

## 2.6 CATALYST CHARACTERISATION METHODS

Catalyst characterization has now become an integral part of catalysis research and is the corner stone in the science of catalysis. Its ultimate goal is to understand the catalytic activity at molecular level, a clear elucidation of the nature of individual catalyst sites and their interdependence and interaction with each other as well as with the reactants.[3] Knowledge of the relationship between preparation method and resulting structural and catalytic properties of solids is a necessary requirement for catalyst design.

Characterization provides information on aspects viz., chemical composition, structure/texture etc. Chemical composition and structure, refers to elemental composition, the structure and proportions of individual phases that may be present, while surface composition means the nature and proportion of functional groups that may be present on the surface. The geometrical structure and morphology i.e. size and shape of crystallites, pore structure, pore volume and total surface area gives information on the texture of the catalyst [4,5]. The catalytic activity is the quantitative measure of the ability of the catalyst to carry out a particular chemical transformation under specified conditions, which also include the selectivity of the catalyst.

### **Chemical resistivity:**

A material to be used for catalytic applications is used in varied environments. Thus, it is a useful study to assess the chemical resistivity/stability in various chemical media. Chemical resistivity in various media – acids ( $H_2SO_4, HNO_3, HCl$ ), bases (NaOH and KOH) and organic solvent media(ethanol, propanol, butanol, benzyl alcohol, 2-ethyl 1-hexanol, anisole, veratrole, acetyl chloride, toluene, benzyl chloride, benzene, xylene, acetone and acetic acid) was studied by taking 500 mg of material in 50 ml of the particular medium and allowing to stand for 24 h. The change in color, nature and weight was observed. Maximum tolerable limits in a particular medium evaluated have been presented through Tables 2.1-2.9. In general the M(IV) phosphates and tungstates are stable in acid and organic solvent media but not so stable in base media.

### **Elemental Analysis:**

Volumetric or gravimetric techniques are well known for obtaining the elemental composition. Wet chemical analyses are routinely done using

suitable procedures for solubilization of a solid and quantitative analysis of the aqueous solutions. Flame photometry, Atomic absorption spectrometry (AAS) or Inductively coupled plasma (ICP) analyzers are commonly used to estimate the chemical composition.

***Inductively Coupled Plasma-Atomic Emission Spectroscopy(ICP-AES):***

ICP-AES, also referred to as Inductively Coupled Plasma Optical Emission Spectrometry (ICP-OES), is an analytical technique used for the detection of trace elements. It is a type of emission spectroscopy that uses the inductively coupled plasma to produce excited atoms and ions that emit electromagnetic radiation at wavelengths characteristic of a particular element. The intensity of this emission is indicative of the concentration of the element within the sample.

In the present study, analysis was performed on a Labtam,8440 Plasmalab, ICP-AES spectrometer. The intensity obtained for each sample is matched against a calibration plot prepared for the particular element for quantitative estimation. The concentration of different elements is actually measured at ppm level, which can be later converted into the % weight of the element, by incorporating the dilution factor. These values are then converted into moles of each element. Elemental analysis of M(IV) phosphates and tungstates is presented through Tables 2.1-2.9.

Elemental analysis shows that the mole ratio of M(IV):P in ZrP, TiP, SnP, ZrPcry, TiPcry SnPcry, and M(IV):W in ZrW, TiW and SnW to be 1:2. Ruthenium was found to be 2.5% in Ru(III)ZrP, Ru(III)TiP, Ru(III)SnP, Ru(III)ZrW, Ru(III)TiW and Ru(III)SnW.

***Ion Exchange Capacity (i.e.c.):***

It is defined as the number of replaceable counter ions per unit mass of the exchanger and is usually expressed as milli-equivalents per gram. The i.e.c of catalysts was determined by measurement of Na<sup>+</sup> ion exchange capacity (IEC) using column method [6]. 500 mg of the acid treated catalyst was transferred to a column. The water inside the column was kept at a level of about 1cm above the material. A 250 ml solution of sodium acetate (0.5 M) was allowed to pass through the column at a flow rate of 0.5ml/min. The effluent was collected in a 500mL conical flask and titrated against standard alkali solution to find out the total H<sup>+</sup> ions eluted. The exchange capacity (in

meq.g<sup>-1</sup>) was evaluated using the formula  $aV/W$ , where  $a$  is molarity and  $V$  the volume of alkali used during titration, and  $W$  is the weight of the catalyst. The Na<sup>+</sup> exchange capacity of all the materials is reported through tables 2.1-2.9. In case of M(IV) phosphates and tungstates under study, the Na<sup>+</sup> exchange capacity follows the order TiPA(3.09)>ZrPA(2.77)>SnPA(1.90) and TiW(1.95)>SnW(1.52)>ZrW(1.32). Since the anion PO<sub>4</sub><sup>3-</sup> or WO<sub>4</sub><sup>2-</sup> is common for the materials under study, the i.e.c. of the various phosphates and tungstates should bear a correlation with the acidity of the cations, viz. Zr<sup>4+</sup>, Sn<sup>4+</sup> and Ti<sup>4+</sup>. Acidity of a cation is related to ion size and charge, the ionic radii for Ti<sup>4+</sup> being (0.74 Å), Zr<sup>4+</sup> (0.86 Å) and Sn<sup>4+</sup> (0.83 Å) [7]. Ti<sup>4+</sup> with smallest ionic radius, the positive charge is concentrated in a small area, increasing the tendency to polarize the O–H bond in the hydroxyl group bonded to it. Thus, i.e.c is also an indicator for protonation ability of a material.

#### ***Thermogravimetric analysis (TGA):***

Thermogravimetry is the measure of quantitative changes in mass occurring in a substance as it undergoes a controlled and programmed heating or cooling as a function of temperature or time. TGA gives an idea about the stability of the material as a function of temperature. Thermal analysis (TGA) was carried out on a Shimadzu thermal analyzer at a heating rate of 10 °C/min.

Thermograms obtained for the materials in question are shown in figures 2.1a – 2.9a. % Weight loss for M(IV) phosphates and tungstates have been presented through Tables 2.1-2.9. All the materials exhibit two weight loss regions. The first region (upto ~180 °C) is attributed to loss of moisture/hydrated water and the second weight loss region above 200 °C is attributed to condensation of structural hydroxyl groups.

#### ***Surface area determination (BET Method):***

The most commonly used methods for estimating the surface area of a material involves physical or chemical adsorption when it starts to level off on pressure increase near the monolayer point. Various adsorbates at different temperatures can be used, depending upon the material characteristic. Measurement of total surface area of a sample requires non-specific physical adsorption [8,9], usually done with simple non-polar molecules like nitrogen

and noble gases. In most cases, nitrogen adsorption method is used, however if metallic species are present, only noble gases like argon and krypton are used exclusively, as nitrogen cannot chemisorb on the metallic surface.

In principle, the total surface area of a material can be divided into the external surface area (the outer side of the particle) and the internal area (contributed by the pores of different dimensions). In case of porous materials, the contribution of the external area is only a fraction of the total surface area and hence, depending upon the nature of the materials, viz., micro, meso or macro porous types, the methodology and considerations for the use of an appropriate model for determining the surface area are important.

In heterogeneous catalysis, surface area of the catalyst plays the most important part and determines potential activity of the catalyst. While comparing the activity of different catalysts or the effect of different pretreatments to a catalyst, the major factor considered is difference in their surface areas rather than their intrinsic activity.

Brunauer, Emmett and Teller (BET) derived the equation for physical adsorption of gases on solid surfaces that leads to multilayer adsorption. The assumptions made are 1) surface is energetically uniform; 2) condensation of layers of gas can proceed to multilayers and 3) adsorbed molecules do not interact laterally.

$$P/V_{\text{ads}} (P^{\circ}-P) = 1/V_m C + P(C-1)/V_m P^{\circ} C$$

where,

$V_{\text{ads}}$  = volume of gas adsorbed at equilibrium pressure

$V_m$  = volume corresponding to monolayer coverage

$P, P^{\circ}$  = saturated vapor pressure of the adsorbate at liquid  $N_2$  temperature

$C$  = isothermal constant given by  $\exp[(H_a-H_1)/RT]$

Where  $H_a$  = enthalpy of adsorption in the first layer

$H_1$  = enthalpy of formation of second and subsequent layers

A plot of  $P/V_{\text{ads}} (P^{\circ}-P)$  versus  $P/P^{\circ}$  is a straight line with the slope  $S = [(C-1)/V_m C]$  and the intercept  $I = [1/V_m C]$ . Knowing  $S$  and  $I$  values  $V_m$  can thus be calculated. The number of gas molecules in a monolayer is multiplied by the cross sectional area of the adsorbate, which gives the total surface area of the solid. This is calculated using the following equation:

$$\text{Specific surface area} = V_m N A_m / 22414 W \text{ m}^2 \text{ g}^{-1}$$

Where,  $N$  is the Avogadro's number,  $W$  is the weight of the catalyst sample in grams,  $A_m$  is the cross sectional area of the adsorbate molecule ( $0.162 \text{ nm}^2$  for  $\text{N}_2$ ) and  $V_m$  is the volume corresponding to monolayer coverage.

Surface area measurement was carried out on Micromeritics Gemini at  $-196^\circ\text{C}$  using nitrogen adsorption isotherms. The surface area values of  $\text{M(IV)}$  phosphates and tungstates and their  $\text{Ru(III)}$  and  $\text{Ru}$  exchanged phases have been presented through Tables 2.1-2.9. For amorphous  $\text{M(IV)}$  phosphates and tungstates the surface area is found to be in the range  $75\text{-}105 \text{ m}^2/\text{g}$ . For crystalline materials the surface area is in the range  $25\text{-}35 \text{ m}^2/\text{g}$ .

BET surface area of  $\text{Ru(III)}$  and  $\text{Ru}$  supported catalysts is found to be in the range  $45\text{-}80 \text{ m}^2/\text{g}$ . Reduction in BET surface area after metal loading can be attributed to pore blockage due to higher size of  $\text{Ru(III)}$  cation.

***Mercury porosimeter method of estimating pore volume:***

A more direct approach to pore size distribution is to measure the volume of liquid (usually mercury as it does not wet most solids) forced under pressure into the capillaries. The effect of interfacial surface tension is to oppose the entry of liquid into the capillary. The force tending to impede the entry of a liquid into a narrow cylindrical radius  $r$  is  $2\pi r \gamma \cos\alpha$ , where  $\alpha$  is the contact angle between liquid and solid and  $\gamma$  is the surface tension. If a pressure  $p$  is imparted to the liquid, the force which tends to drive mercury into pores is  $\pi r^2 p$ . Equating these two forces gives,  $r = 2\gamma \cos\alpha / p$  as the radius of a pore which will accept the liquid driven in at a pressure  $p$ . For mercury, a contact angle of  $140^\circ$  and a surface tension of  $4.8 \times 10^{-3} \text{ Nm}^{-1}$  are typical values. The above equation indicates that a pressure of  $60000 \text{ psi}$  must be applied to fill pores of  $15 \text{ \AA}$  radius. A pressure greater than this, in ordinary circumstances is impracticable, so that the mercury porosimeter suffers from disadvantage that capillaries of radius less than  $30 \text{ \AA}$  remain unfilled and escape detection. Nevertheless, since large pores are accounted for easily the porosimeter is useful in investigating the pore volume, pore size distribution and percentage porosity of porous materials containing pores up to about  $15 \text{ \AA}$  radius.

Pore volume and pore size distribution measurement was carried out on Micromeritics Auto pore 9500. Pore volume and total pore area of M(IV) phosphates and tungstates have been presented through Tables 2.1-2.9.

***Determination of surface acidity by temperature programmed desorption (TPD) studies:***

Determining the quantity and strength of the acid sites is crucial to understanding and predicting the performance of a catalyst. Temperature-Programmed Desorption (TPD) is one of the most widely used and flexible techniques for characterizing the acid sites on surfaces.

Temperature programmed desorption (TPD), also known as Thermal desorption spectroscopy (TDS) is the method of observing desorbed molecules from a surface when the surface temperature is increased. Many researchers prefer the name TPD because it is not a spectroscopic method.

When molecules come in contact with a surface, they adsorb onto it, minimizing their energy by forming a chemical bond with the surface. The binding energy varies with the combination of the adsorbate and surface. If the surface is heated, at one point, the energy transferred to the adsorbed species will cause it to desorb. The temperature at which this happens is known as the desorption temperature. Thus TPD gives information on the binding energy.

There are three types of molecular probes commonly used for characterizing acid sites using TPD:

- ❖ Ammonia
- ❖ Non-reactive vapours
- ❖ Reactive vapours

Larger non-reactive amines such as pyridine and t-butyl amine are often preferable alternatives to ammonia because their size permits access to the pore size range required for catalytic cracking reactions and they titrate only the strong and moderate acid sites. The most common application for these probes is the characterization of pyridine adsorption by infrared spectroscopy. However, the determination of extinction coefficients is difficult and IR of pyridine is typically used in a qualitative manner, rather than as a

measurement of site densities. TPD of ammonia is a widely used method for characterization of site densities in solid acids due to the simplicity of the technique. Also, ammonia is a very basic molecule which is capable of titrating weak acid sites which may not contribute to the activity of catalysts. The strongly polar adsorbed ammonia is also capable of adsorbing additional ammonia from the gas phase.

In the present work, the acidity of different catalysts has been determined using the TPD of ammonia. This method involves three steps. The sample is first degassed and then saturated with a mixture of 5% NH<sub>3</sub>+He gas at 120 °C. Ammonia gets chemisorbed on the acidic sites of the catalyst. After removal of any physisorbed ammonia from the surface by purging He at 120°C for 30 min, the temperature programmed desorption is carried out at a heating rate of 10 °C/ min. The desorbed gas concentration is continuously monitored and recorded with temperature by a thermal conductivity detector (TCD). This concentration-temperature plot is referred to as the TPD profile. The area under the profile is proportional to the amount of gas desorbed. Acid sites with varying acid strength differ in their heat of adsorption, which is reflected in the TPD profile by way of a number of distinct peaks representing the acid sites of the catalyst. The acidity is reported as mmol/gm.

NH<sub>3</sub> TPD was carried out on Micromeritics Chemisorb 2720. Ammonia was chemisorbed at 120°C and then desorption was carried out up to 700°C at a heating rate of 10°C/min.

TPD patterns of the materials in question are presented through Figures 2.1b-2.9b. The area under the curve indicates the amount of NH<sub>3</sub> desorbed and hence the number of surface acid sites. In general, amorphous materials exhibit broad desorption peak compared to crystalline ones. Though the crystalline materials show sharper peaks indicating less number of acid sites, the desorption temperatures of NH<sub>3</sub> are high indicating strong acid sites. Acidity of a cation and hence surface acidity depends on the size and charge of the cation. In the materials under study Zr, Ti and Sn all being tetravalent as well as bearing a common anion phosphate/tungstate the size of the cation [Ti<sup>+4</sup>(0.74 Å<sup>0</sup>), Zr<sup>+4</sup>(0.86 Å<sup>0</sup>), Sn<sup>+4</sup>(0.83 Å<sup>0</sup>)] [7] seems to play a dominant role.

**X-ray diffraction studies:**

X-ray powder diffraction is a standard tool for the identification and characterization of crystalline solid phases. It gives information on the geometry of the crystal lattice, specific atoms and their arrangement in the unit cell of crystal structure. It is most effective in structure determination when the compound to be investigated is in a single phase. There are conventionally two types of diffraction studies performed using X-rays: 1) Single crystal diffraction and 2) Powder X-ray diffraction (PXRD). In comparison to the information obtained by single crystal intensity data, the PXRD profiles yield far poorer information mainly due to equivalent and overlapping reflections. Compared to the three dimensional location of each reflection in a single crystal diffraction experiment, the powder diffraction pattern can give only one dimensional data, due to the rotational projection of the randomly oriented reciprocal lattices. PXRD is a long-range order technique sensitive to the basic periodic structure of a solid sample.

Any diffraction pattern consists of: peak position ( $2\theta$ ), peak intensity (cps) and the nature of the peak (broad or sharp). The peak positions are dependent on the geometry of the crystal lattice i.e. size and shape of the unit cell. The intensities of the peaks in a profile are related to the specific atoms in a crystal and their arrangement in the unit cell of the crystal. The shape of the peak is related to the size and the perfection of the crystallites and various instrumental parameters. The diffraction profile obtained through constructive interference, obeys Bragg's law

$$n \lambda = 2d \sin \theta$$

where,  $n$  = order of diffraction

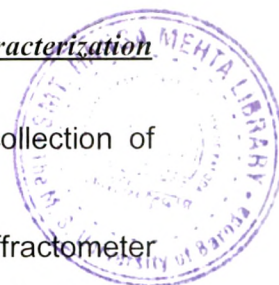
$\lambda$  = wavelength of incident X-ray (in Å)

$d$  = distance between two parallel scattering planes (in Å)

$\theta$  = incident angle

A plot of cps v/s  $2\theta$  is obtained where,  $2\theta$  is an experimental parameter (angle between the diffracted and the undeviated X-ray waves).

Phase identification is done by comparison of the pattern with the data base-powder diffraction files distributed by International Center for diffraction



data (ICDD), (Formerly ASTM and then JCPDS), which is a collection of single phase X-ray diffraction patterns in the form of tables.

X-ray diffractogram ( $2\theta = 4-60^\circ$ ) was obtained on X-ray diffractometer (Rigaku Dmax 2200) with Cu- $K_\alpha$  radiation and nickel filter. Typical diffractograms obtained are presented in figure 2.1c-2.9c. The absence of peaks in the X-ray diffractogram for ZrP, SnP, TiP, ZrW, SnW and TiW indicates the amorphous nature of the materials. In case of ZrPcry, SnPcry and TiPcry sharp peaks are obtained confirming the crystalline nature of the material. The crystalline phases were confirmed from the JCPDS files database .

#### ***Infrared Spectroscopy (FTIR):***

Infrared spectroscopy is based on the interaction of electromagnetic radiation with matter. Every solid, liquid or gaseous material is built up of aggregates of molecules or periodic lattice of well-defined molecules or atoms. Majority of such systems of matter exhibit local or global dipole moment depending upon masses, binding forces, distances and relative angle of atoms, which make up molecules. Each of these has a set of characteristic vibrational states, which are typical of a material. The various properties of a material are dependent upon its microstructure, which can be understood from IR spectra of the material. Vibrational spectroscopy is the most promising and widely used method for material characterization. The advantage being that, detailed microstructural information is obtained from the vibrational spectra. The information obtained from IR spectra serves both complementary and supplementary to those obtained from other techniques like XRD, e.g. information regarding phase transition, compositional changes or presence of surface functional groups in a material. Most of the limitations of other methods are overcome in the application of IR spectroscopy to study the surface of solid materials.

In the present study, the IR absorption spectra of the synthesized materials were recorded to obtain information regarding the functional groups present in the material.

FTIR spectra of M(IV) phosphates and tungstates were recorded using KBr wafer on a Bomem MB series with Epson Hi 80 printer/plotter. The FTIR spectra for all the materials are presented through figures 2.1d–2.9d.

The FTIR spectra of M(IV) phosphates (ZrP, SnP, TiP, Zrpcry, Snpcry and Tipcry) and tungstates (ZrW, SnW and TiW) exhibits a broad band in the region  $\sim 3400\text{cm}^{-1}$  which is attributed to asymmetric and symmetric –OH stretches. A sharp medium band at  $\sim 1635\text{cm}^{-1}$  is attributed to aquo (H–O–H) bending. For M(IV) phosphates, a band in the region  $\sim 1035\text{cm}^{-1}$  is attributed to the presence of P=O stretching. A medium intensity band at  $1400\text{cm}^{-1}$  is attributed to the presence of  $\delta(\text{POH})$ .

***Scanning Electron Microscopy (SEM):***

It is a type of electron microscopy capable of producing high resolution images of a sample surface. Electron microscopes use a beam of highly energetic electrons to examine objects on a very fine scale. Due to the manner in which the image is created, SEM images have a characteristic three-dimensional appearance and are useful for judging the surface structure of the sample. In a typical SEM, electrons are thermionically emitted from a tungsten or lanthanum hexaboride ( $\text{LaB}_6$ ) cathode and are accelerated towards an anode; alternatively electrons can be emitted via field emission (FE). The electron beam, which typically has an energy ranging from a few hundred eV to 50 keV, is focused by one or two condenser lenses into a beam with a very fine focal spot sized 1 nm to 5 nm. The beam passes through pairs of scanning coils in the objective lens, which deflect the beam over a rectangular area of the sample surface. Through these scattering events, the primary electron beam, effectively spreads and fills a teardrop-shaped volume, known as the interaction volume, extending from less than 100 nm to around 5  $\mu\text{m}$  into the surface. Interactions in this region lead to the subsequent emission of electrons which are then detected to produce an image. The most common imaging mode monitors low energy (<50 eV) secondary electrons. Due to their low energy, these electrons originate within a few nanometers from the surface. The electrons are detected by a scintillator-photomultiplier device and the resulting signal is rendered into a two-dimensional intensity distribution, that can be viewed and saved as a

digital image. The brightness of the signal, depends on the number of secondary electrons reaching the detector. If the beam enters the sample, perpendicular to the surface, then the activated region is uniform about the axis of the beam and a certain number of electrons "escape" from within the sample. As the angle of incidence increases, the "escape" distance of one side of the beam will decrease and more secondary electrons will be emitted. Thus, steep surfaces and edges tend to be brighter than flat surfaces, which results in images with a well-defined, three-dimensional appearance. Using this technique, resolutions less than 1 nm are possible. In addition to the secondary electrons, backscattered electrons can also be detected. Backscattered electrons may be used to detect contrast between areas with different chemical compositions. These can be observed especially when the average atomic number of the various regions is different.

SEM were scanned on Jeol JSM-5610-SLV scanning electron microscope.

SEM of M(IV) phosphates and tungstates have been presented though figures 2.1e-2.9e. SEM of Ru supported M(IV) phosphates and tungstates are presented through Figures 2.1f-2.6f.

**Table 2.1 Characterisation of ZrP**

Characterization			
Chemical resistivity (maximum tolerable limits)	36N H <sub>2</sub> SO <sub>4</sub> , 16N HNO <sub>3</sub> , 10N HCl, 5N NaOH, 5N KOH, organic media (ethanol, propanol, butanol, benzyl alcohol, 2-ethyl 1-hexanol, anisole, veratrole, acetyl chloride, toluene, benzyl chloride, benzene, xylene acetone and acetic acid).		
Elemental analysis(ICP-AES)	Zr wt. %	P wt. %	
	20.15	13.69	
Ion Exchange capacity	2.77 meq./g		
TGA	Temperature range (°C)	% Weight loss	
	40-180	2.27	
	200-500	8.51	
Surface area(BET method, m <sup>2</sup> /g )	ZrP	Ru(III)ZrP	RuZrP
	81.90	69.20	71.10
Pore volume (ml/g)	0.70		
Total pore area (m <sup>2</sup> /g)	117.8		
Surface acidity	2.34 mmol/g		
X ray Diffraction	Amorphous		
FTIR	~3400cm <sup>-1</sup> (b) asymmetric and symmetric –OH stretches. ~1635cm <sup>-1</sup> (s) aquo (H–O–H) bending ~1035cm <sup>-1</sup> (m) P=O stretching. ~ 1400cm <sup>-1</sup> (m) δ(POH).		
SEM	Irregular morphology		

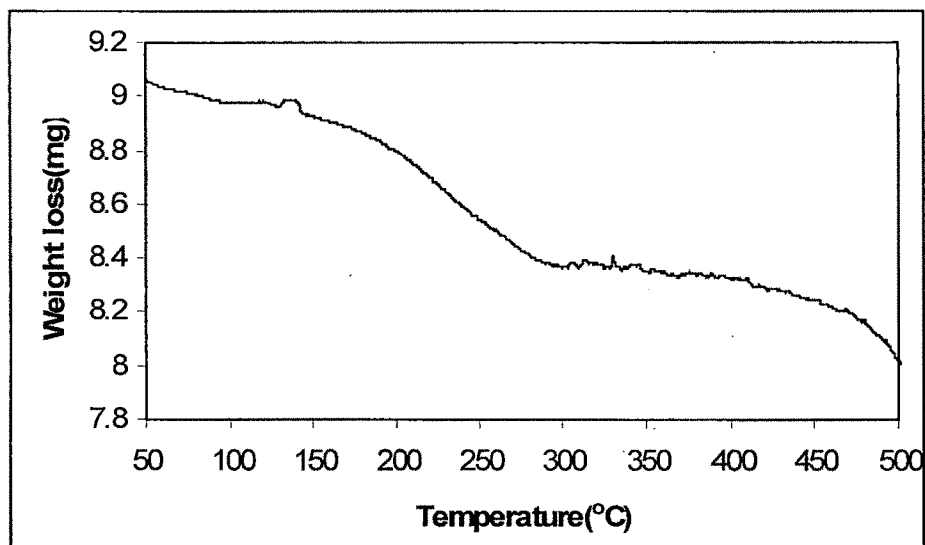


Figure 2.1a TGA of ZrP

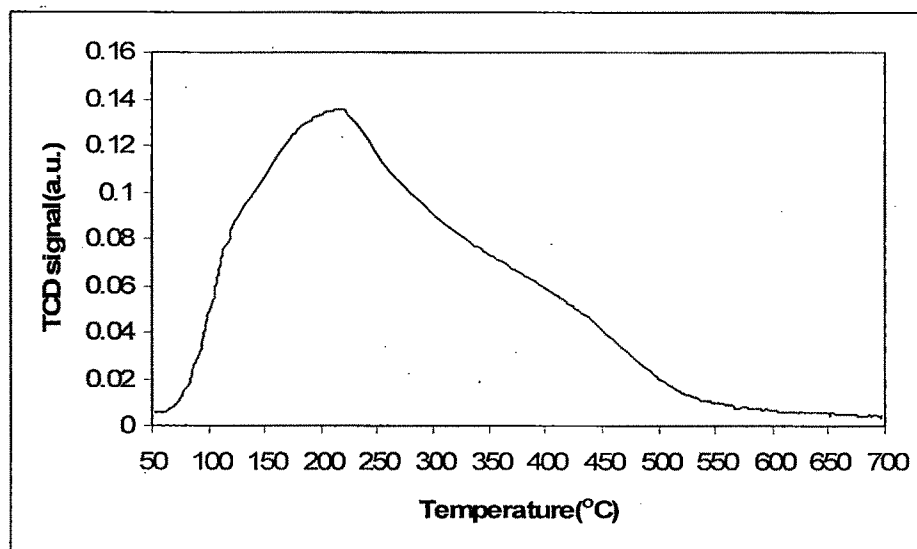
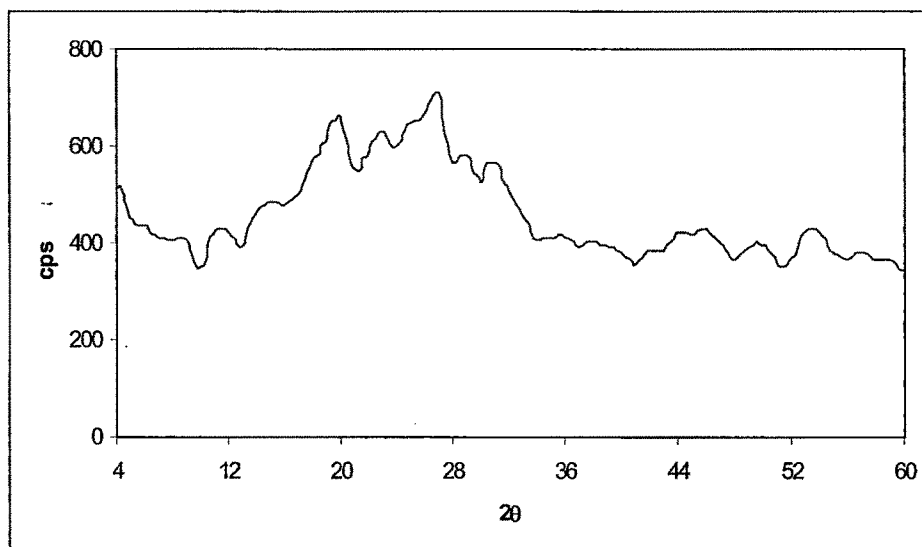
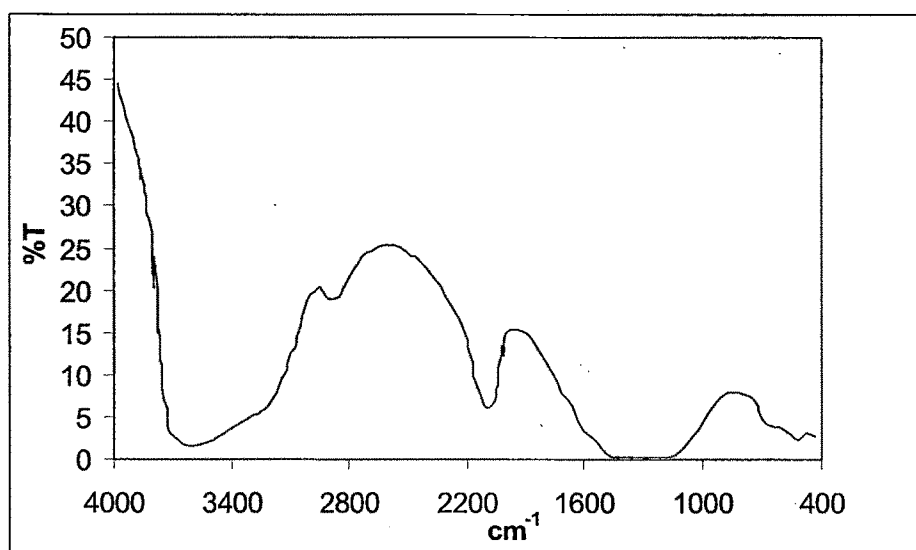


Figure 2.1b TPD pattern of ZrP



*Figure 2.1c XRD of ZrP*



*Figure 2.1d FTIR of ZrP*

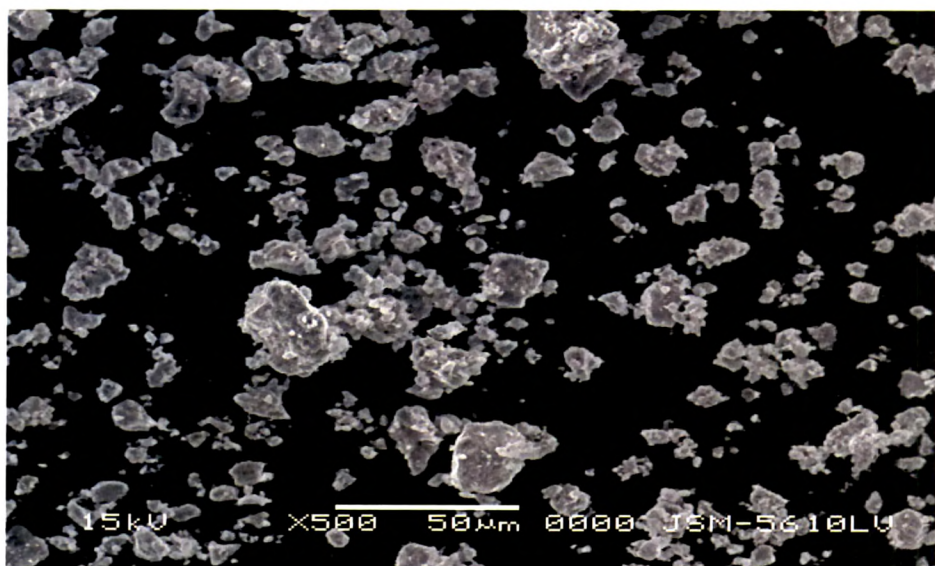


*Figure 2.1e SEM of ZrP*

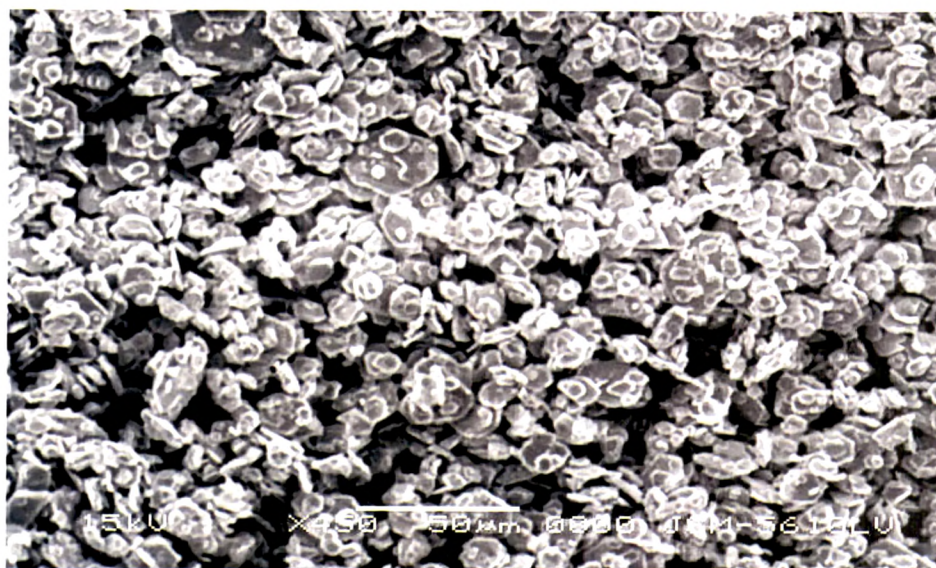


*Figure 2.1f SEM of Ru ZrP*

**Table 2.2 Characterisation of TiP**

Characterization			
Chemical resistivity (maximum tolerable limits)	36N H <sub>2</sub> SO <sub>4</sub> , 16N HNO <sub>3</sub> , 10N HCl, 5N NaOH, 5N KOH, organic media (ethanol, propanol, butanol, benzyl alcohol, 2-ethyl 1-hexanol, anisole, veratrole, acetyl chloride, toluene, benzyl chloride, benzene, xylene acetone and acetic acid).		
Elemental analysis(ICP-AES)	Ti wt. %	P wt. %	
	21.88	28.32	
Ion Exchange capacity	3.09 meq./g		
TGA Weight loss%,	Temperature range (°C)	% Weight loss	
	40-180	7.5	
	200-500	1.8	
Surface area(BET method, m <sup>2</sup> /g)	TiP	Ru(III)TiP	RuTiP
	75.45	55.22	51.32
Pore volume (ml/g)	0.87		
Total pore area (m <sup>2</sup> /g)	30.48		
Surface acidity	0.59 mmol/g		
X ray Diffraction	Amorphous		
FTIR	~3400cm <sup>-1</sup> (b) asymmetric and symmetric –OH stretches. ~1635cm <sup>-1</sup> (s) aquo (H–O–H) bending ~1035cm <sup>-1</sup> (m) P=O stretching. ~ 1400cm <sup>-1</sup> (m) δ(POH)		
SEM	Irregular morphology		

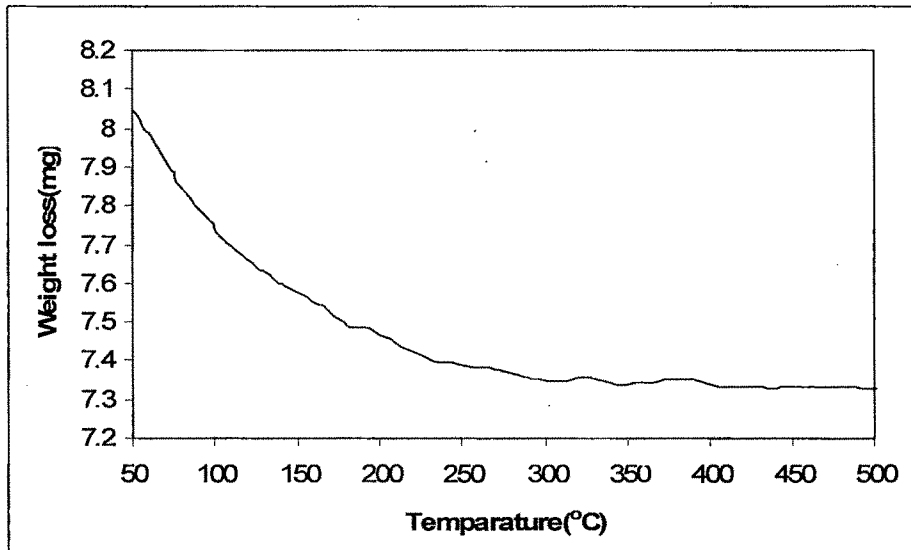


Figure 2.2a TGA of TIP

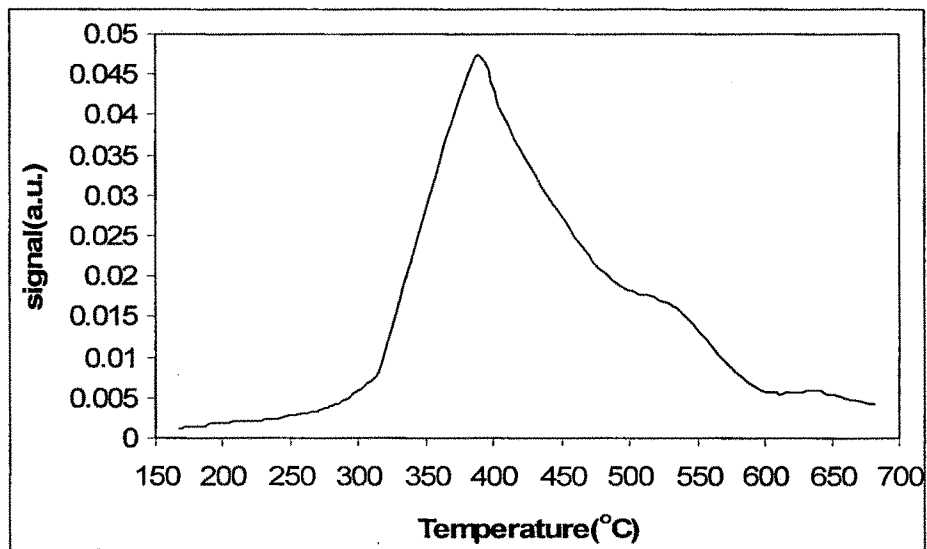


Figure 2.2b TPD pattern of TIP

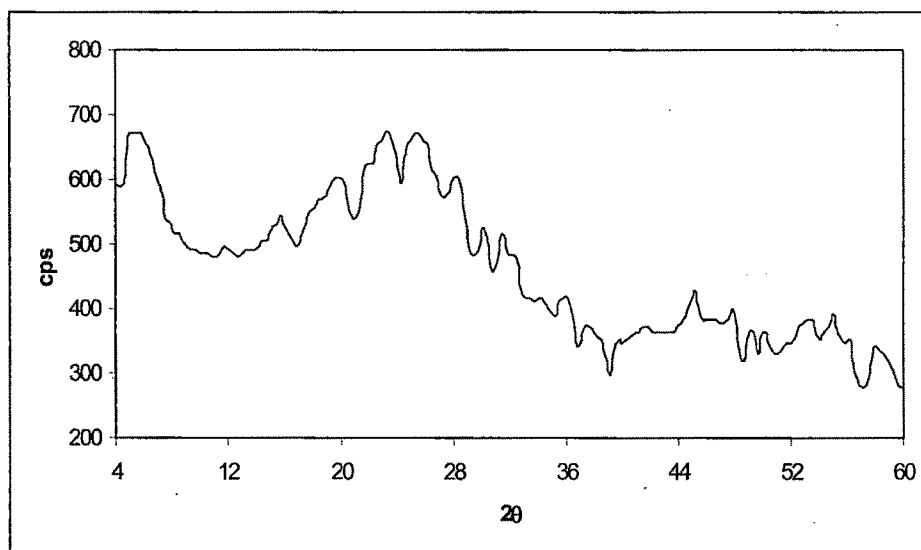


Figure 2.2c XRD of TiP

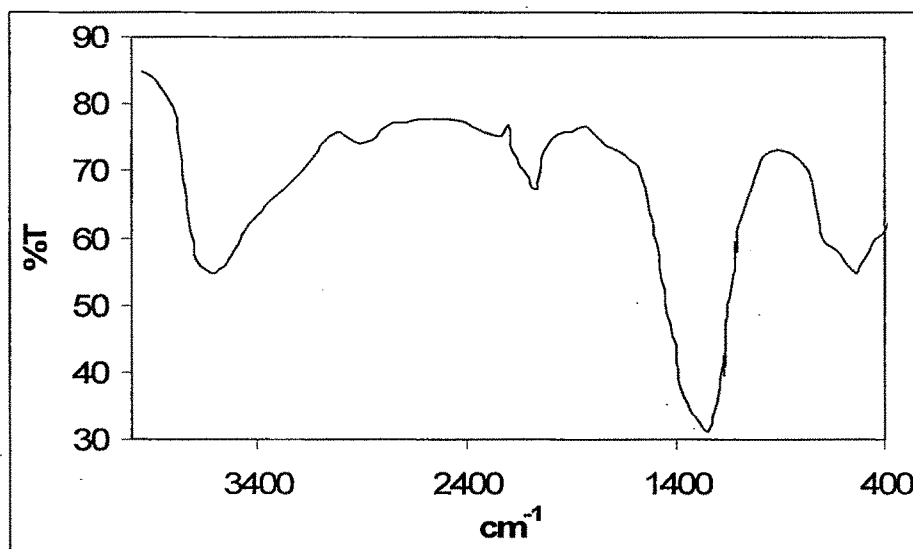
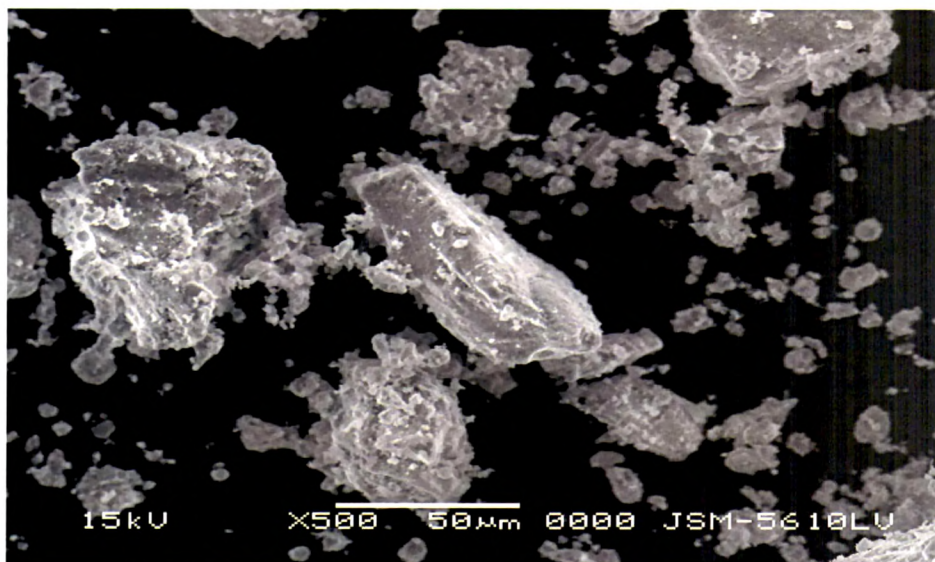
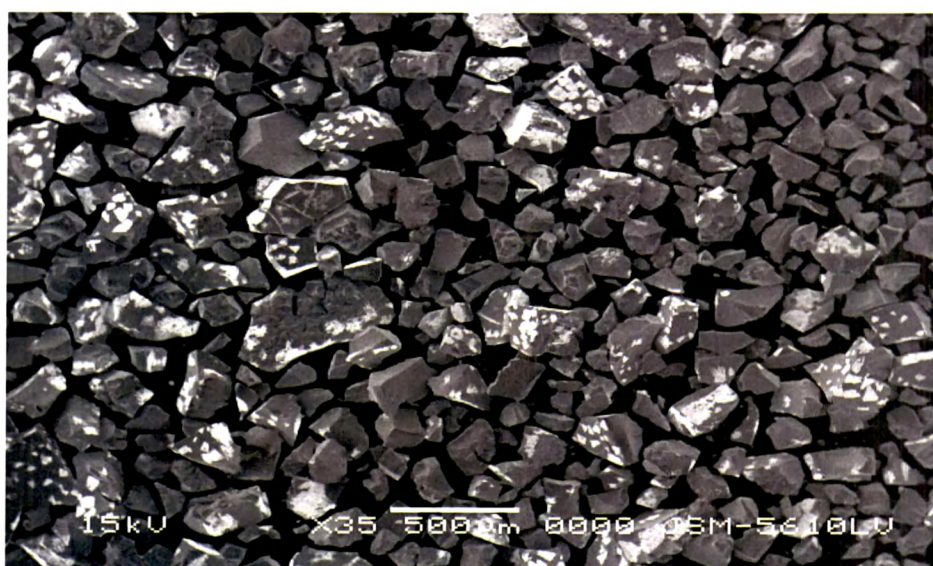


Figure 2.2d FTIR of TiP



*Figure 2.2e SEM of TiP*



*Figure 2.2f SEM of Ru TiP*

**Table 2.3 Characterisation of SnP**

Characterization			
Chemical resistivity (maximum tolerable limits)	36N H <sub>2</sub> SO <sub>4</sub> , 16N HNO <sub>3</sub> , 10N HCl, 5N NaOH, 5N KOH, organic media (ethanol, propanol, butanol, benzyl alcohol, 2-ethyl 1-hexanol, anisole, veratrole, acetyl chloride, toluene, benzyl chloride, benzene, xylene acetone and acetic acid).		
Elemental analysis(ICP-AES)	Sn wt. %	P wt. %	
	26.70	13.92	
Ion Exchange capacity	2.96 meq./g		
TGA	Temperature range (°C)	% Weight loss	
	40-180	7.3	
	200-500	2.27	
Surface area(BET method, m <sup>2</sup> /g)	SnP	Ru(III)SnP	RuSnP
	98.55	72.22	73.44
Pore volume (ml/g)	0.28		
Total pore area (m <sup>2</sup> /g)	38.92		
Surface acidity	1.81mmol/g		
X ray Diffraction	Amorphous		
FTIR	~3400cm <sup>-1</sup> (b) asymmetric and symmetric –OH stretches. ~1635cm <sup>-1</sup> (s) aquo (H–O–H) bending ~1035cm <sup>-1</sup> (m) P=O stretching. ~ 1400cm <sup>-1</sup> (m) δ(POH).		
SEM	Irregular morphology		

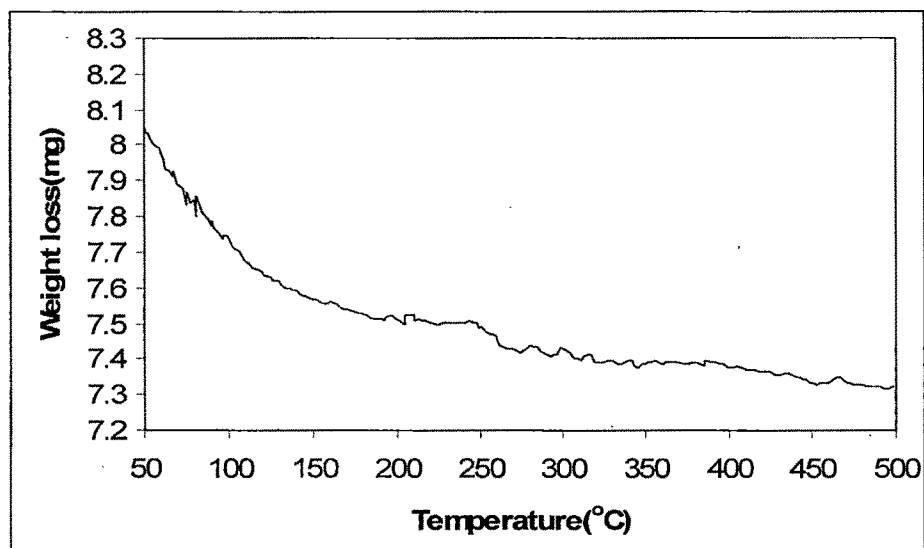


Figure 2.3a TGA of SnP

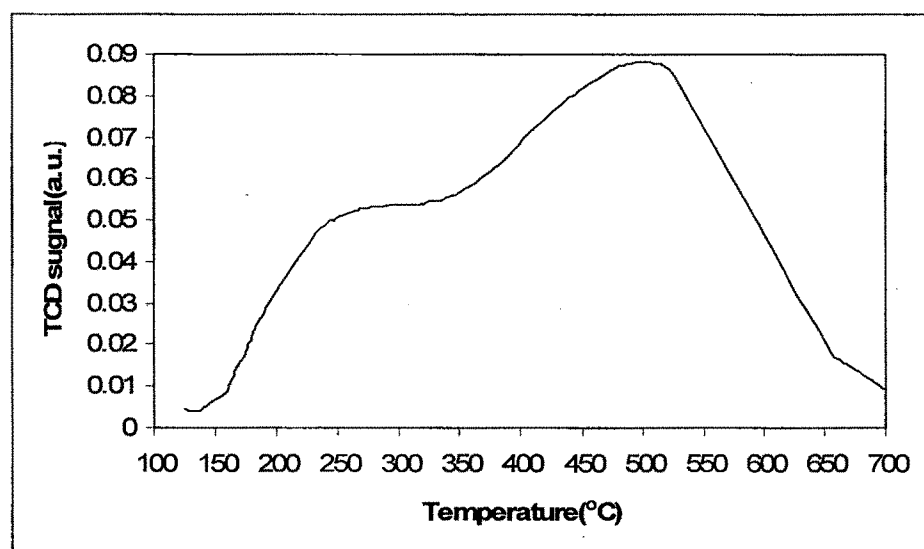


Figure 2.3b TPD pattern of SnP

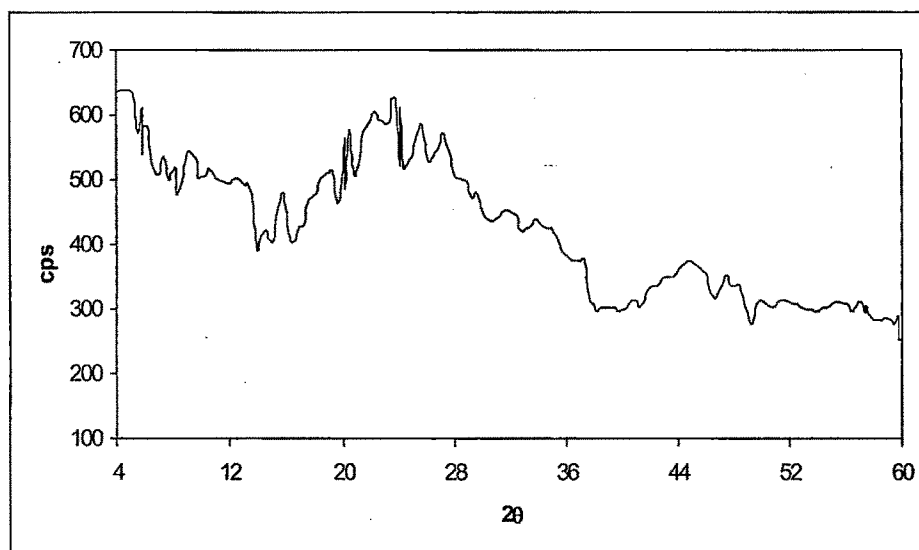


Figure 2.3c XRD of SnP

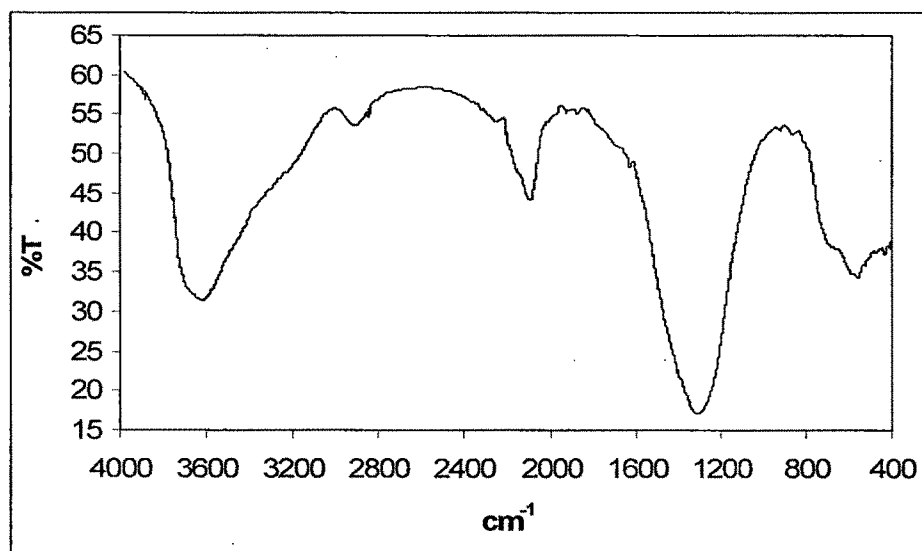
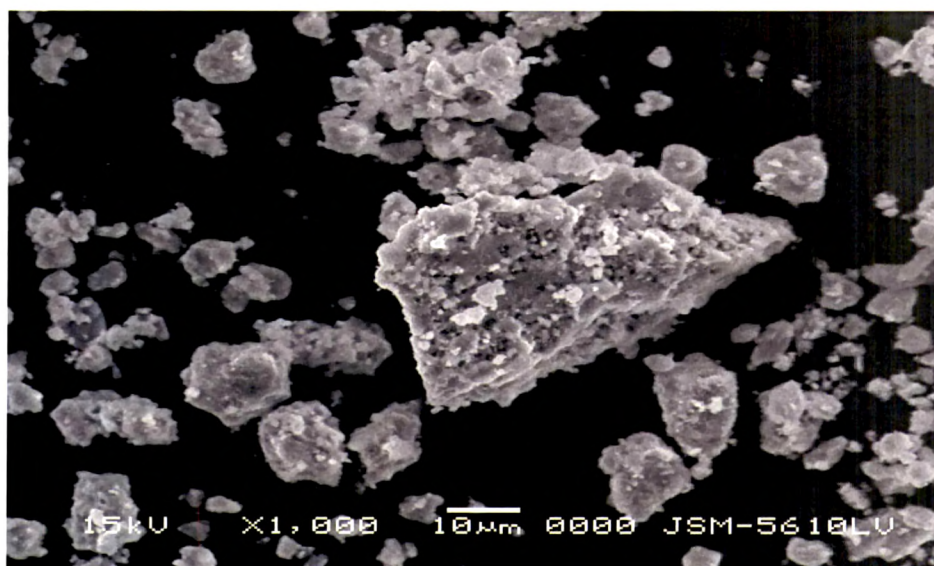
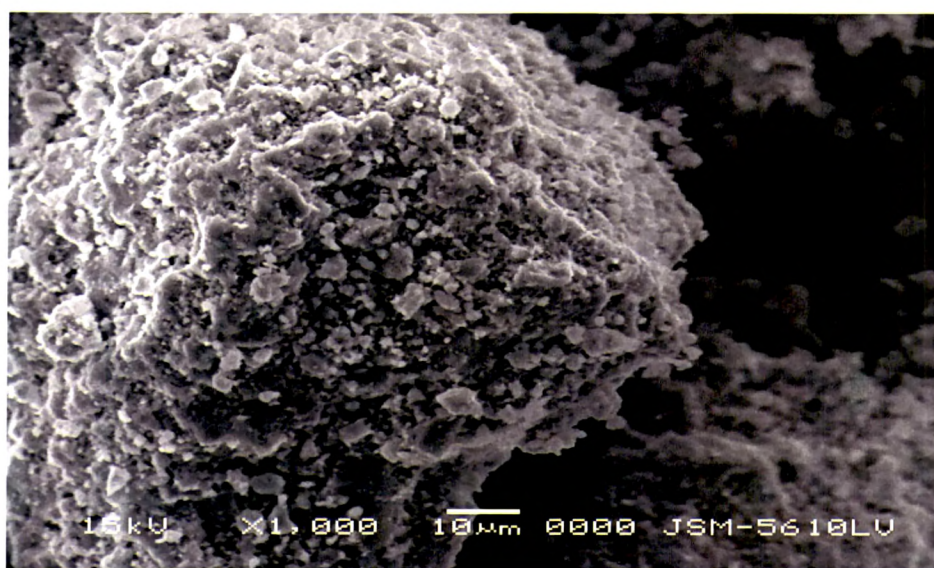


Figure 2.3d FTIR of SnP



*Figure 2.3e SEM of SnP*



*Figure 2.3f SEM of Ru SnP*

**Table 2.4 Characterisation of ZrW**

Characterization			
Chemical resistivity (maximum tolerable limits)	36N H <sub>2</sub> SO <sub>4</sub> , 16N HNO <sub>3</sub> , 10N HCl, 4N NaOH, 4N KOH, organic media (ethanol, propanol, butanol, benzyl alcohol, 2-ethyl 1-hexanol, anisole, veratrole, acetyl chloride, toluene, benzyl chloride, benzene, xylene acetone and acetic acid)		
Elemental analysis(ICP-AES)	Zr wt. %	W wt. %	
	8.21	32.74	
Ion Exchange capacity	1.32 meq./g		
TGA Weight loss%,	Temperature range (°C)	% Weight loss	
	40-180	6.33	
	200-500	2.37	
Surface area(BET method, m <sup>2</sup> /g)	ZrW	Ru(III)ZrW	RuZrW
	73.11	46.21	44.53
Mercury porosimetry	Pore volume (ml/g)	Total pore area (m <sup>2</sup> /g)	
	0.23	15.26	
NH <sub>3</sub> TPD	0.64 mmol/g		
X ray Diffraction	Amorphous		
FTIR	~3400cm <sup>-1</sup> (b) asymmetric and symmetric –OH stretches ~1635cm <sup>-1</sup> (s) aquo (H–O–H) bending		
SEM	Irregular morphology		

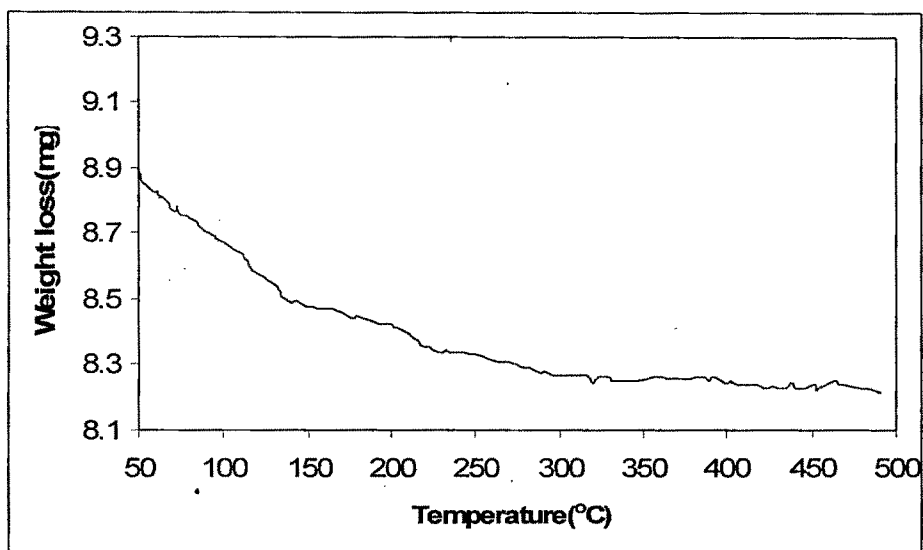


Figure 2.4a TGA of ZrW

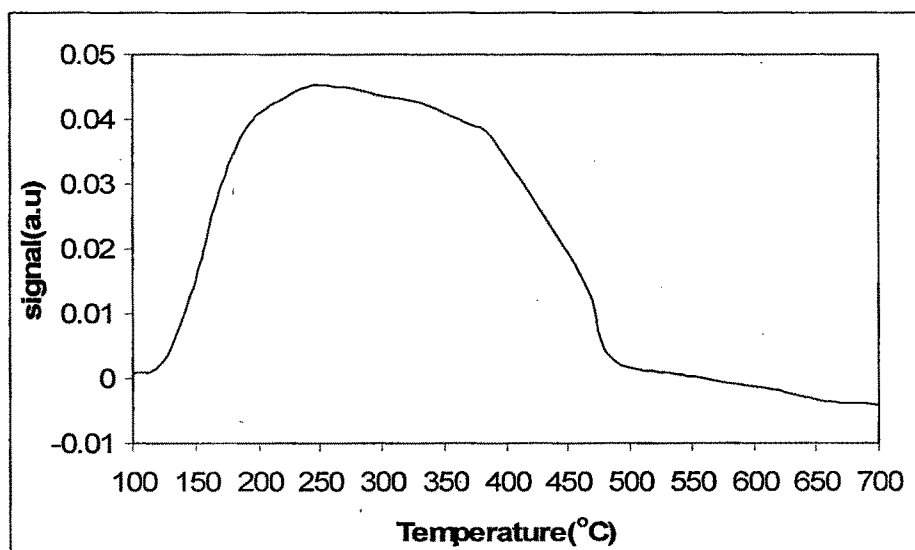
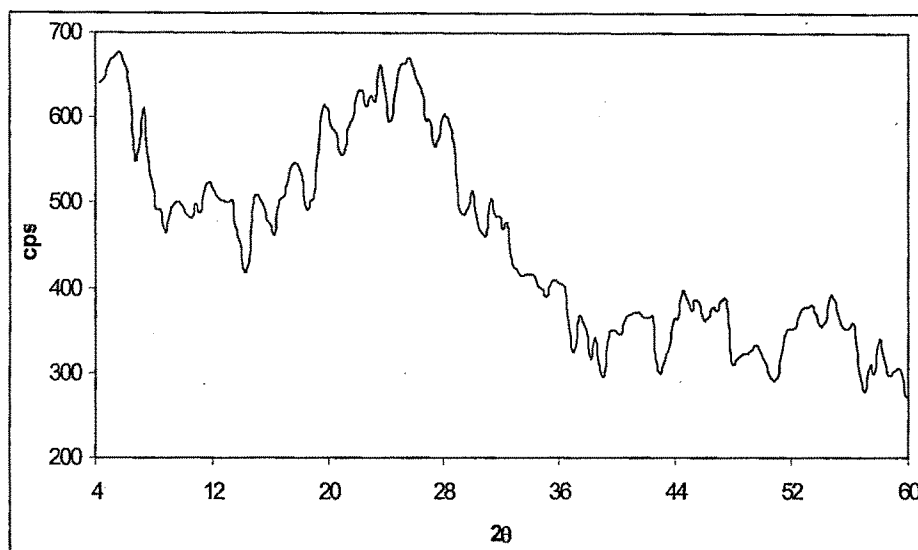
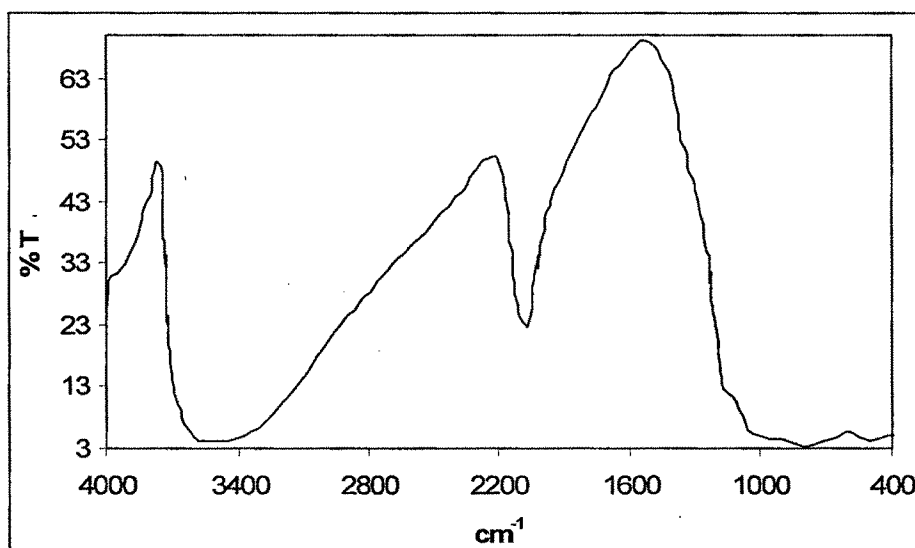


Figure 2.4b TPD pattern of ZrW



*Figure 2.4c XRD of ZrW*



*Figure 2.4d FTIR of ZrW*



*Figure 2.4e SEM of ZrW*



*Figure 2.4f SEM of Ru ZrW*

**Table 2.5 Characterisation of TiW**

Characterization			
Chemical resistivity (maximum tolerable limits)	36N H <sub>2</sub> SO <sub>4</sub> , 16N HNO <sub>3</sub> , 10N HCl, 5N NaOH, 5N KOH, organic media (ethanol, propanol, butanol, benzyl alcohol, 2-ethyl 1-hexanol, anisole, veratrole, acetyl chloride, toluene, benzyl chloride, benzene, xylene acetone and acetic acid).		
Elemental analysis(ICP-AES)	Ti wt. %	W wt. %	
	5.44	41.64	
Ion Exchange capacity	1.95 meq./g		
TGA	Temperature range (°C)	% Weight loss	
	40-180	8.45	
	200-500	2.67	
Surface area(BET method, m <sup>2</sup> /g)	TiW	Ru(III)TiW	RuTiW
	107.75	89.45	85.70
Pore volume (ml/g)	0.86		
Total pore area (m <sup>2</sup> /g)	28.58		
Surface acidity	0.89mmol/g		
X ray Diffraction	Amorphous		
FTIR	~3400cm <sup>-1</sup> (b) asymmetric and symmetric –OH stretches ~1635cm <sup>-1</sup> (s) aquo (H–O–H) bending		
SEM	Irregular morphology		

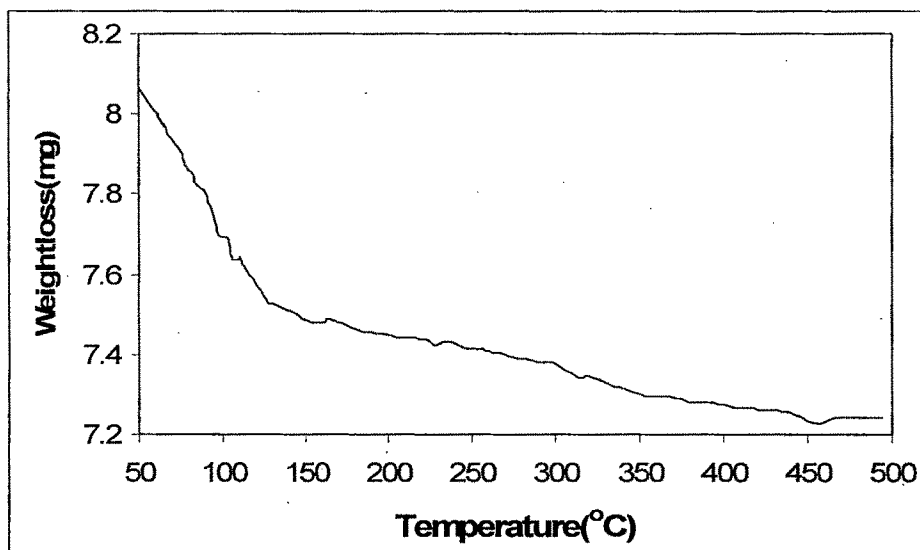


*Figure 2.5.a TGA of TiW*

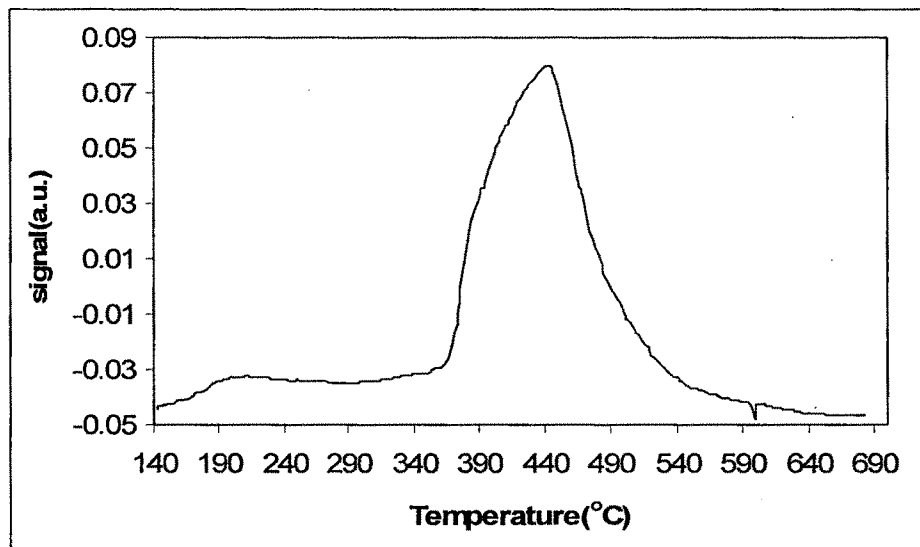


*Figure 2.5.b TPD pattern of TiW*

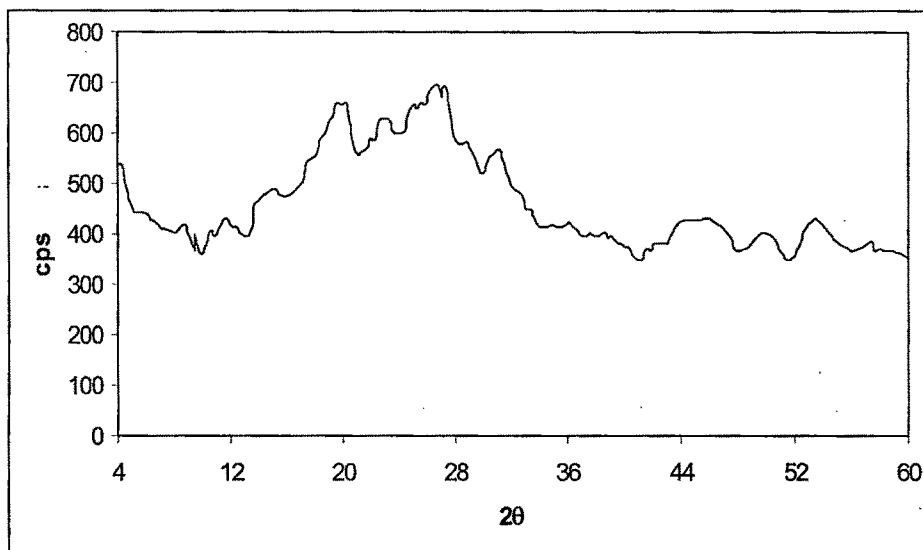


*Figure 2.5c XRD of TiW*

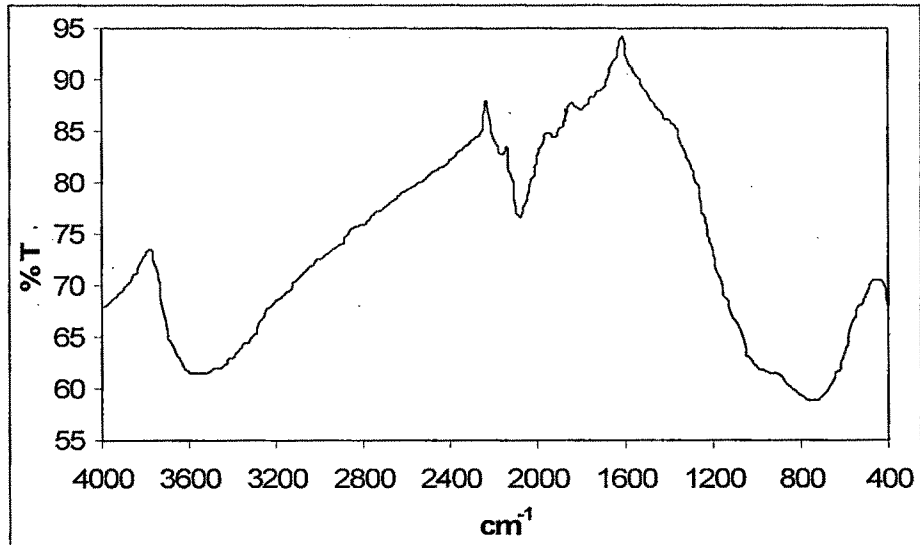


*Figure 2.5.d FTIR of TiW*

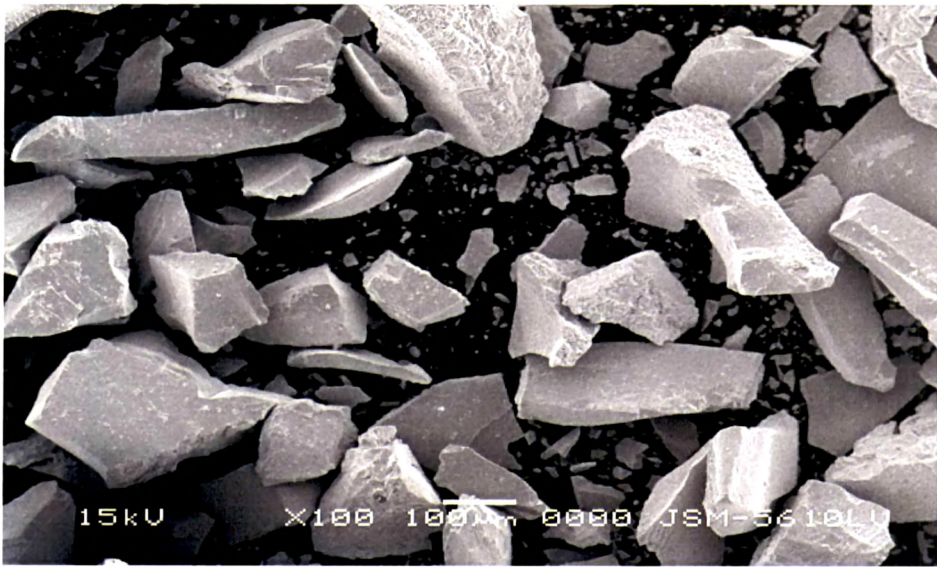


*Figure 2.5e SEM of TiW*



*Figure 2.5f SEM of Ru TiW*

**Table 2.6 Characterisation of SnW**

Characterization			
Chemical resistivity (maximum tolerable limits)	36N H <sub>2</sub> SO <sub>4</sub> , 16N HNO <sub>3</sub> , 10N HCl, 4N NaOH, 4N KOH, organic media (ethanol, propanol, butanol, benzyl alcohol, 2-ethyl 1-hexanol, anisole, veratrole, acetyl chloride, toluene, benzyl chloride, benzene, xylene acetone and acetic acid).		
Elemental analysis(ICP-AES)	Sn wt. %	W wt. %	
	9.67	29.79	
Ion Exchange capacity	1.52 meq./g		
TGA	Temperature range (°C)	% Weight loss	
	40-180	7.37	
	200-500	3.52	
Surface area(BET method, m <sup>2</sup> /g)	SnW	Ru(III)SnW	RuSnW
	87.33	59.20	55.12
Mercury porosimetry	Pore volume (ml/g)	Total pore area (m <sup>2</sup> /g)	
	0.24	22.48	
NH <sub>3</sub> TPD	0.77 mmol/g		
X ray Diffraction	Amorphous		
FTIR	~3400cm <sup>-1</sup> (b) asymmetric and symmetric –OH stretches ~1635cm <sup>-1</sup> (s) aquo (H–O–H) bending		
SEM	Irregular morphology		

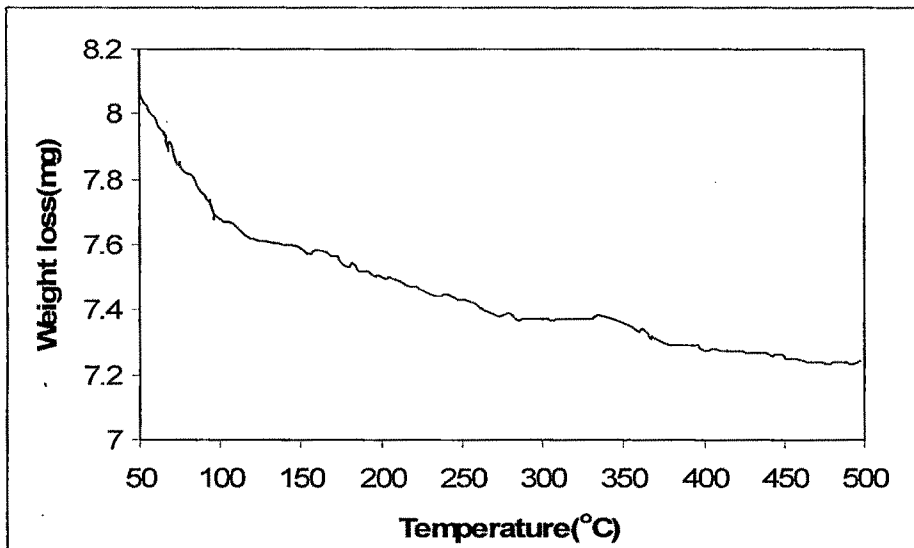


*Figure 2.6a TGA of SnW*

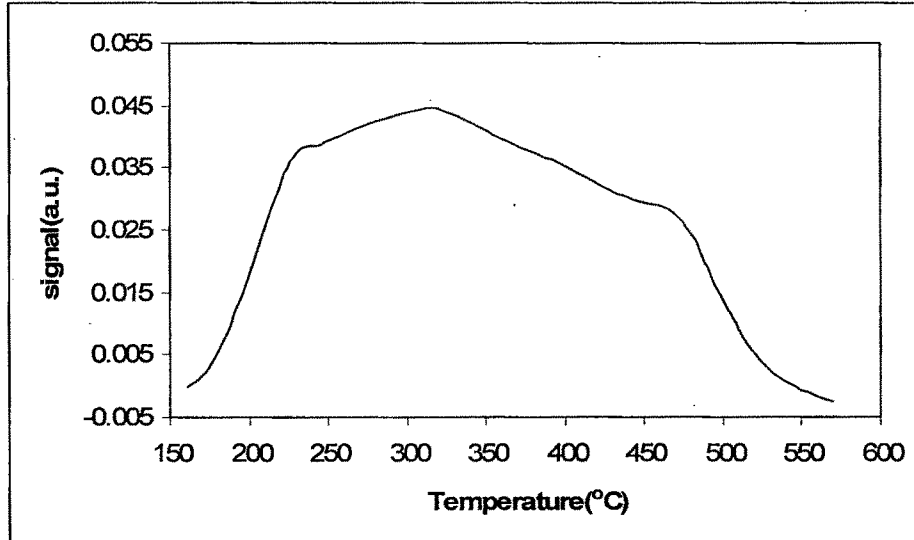


*Figure 2.6b TPD pattern of SnW*

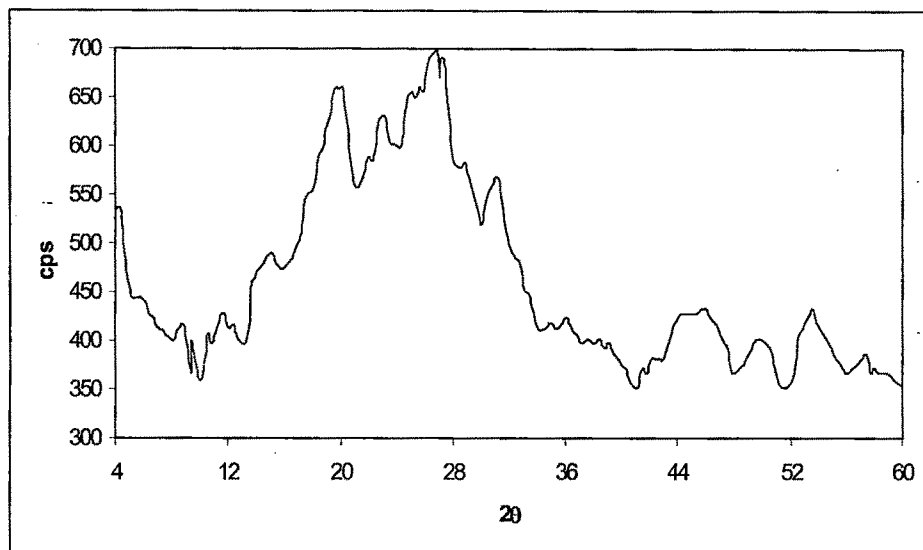


Figure 2.6c XRD of SnW

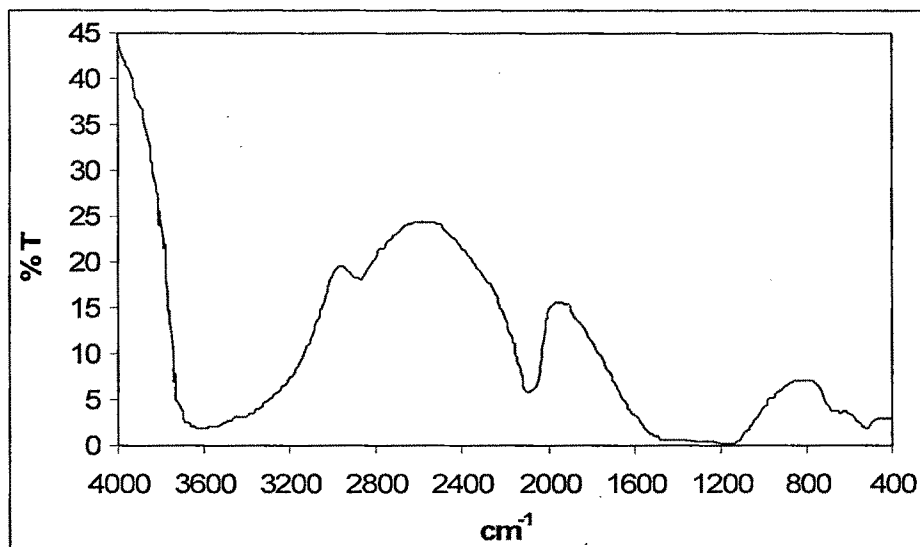
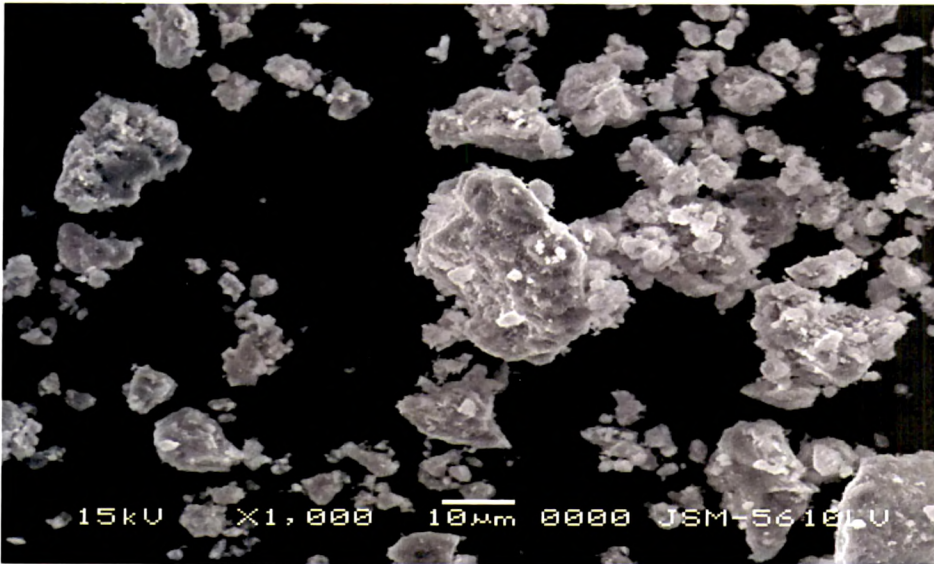


Figure 2.6d FTIR of SnW



*Figure 2.6e SEM of SnW*



*Figure 2.6f SEM of Ru SnW*

**Table 2.7 Characterisation of ZrP<sub>cry</sub>**

Characterization		
Chemical resistivity (maximum tolerable limits)	36N H <sub>2</sub> SO <sub>4</sub> , 16N HNO <sub>3</sub> , 10N HCl, 5N NaOH, 5N KOH, organic media (ethanol, propanol, butanol, benzyl alcohol, 2-ethyl 1-hexanol, anisole, veratrole, acetyl chloride, toluene, benzyl chloride, benzene, xylene acetone and acetic acid).	
Elemental analysis(ICP-AES,Zr:P ratio)	Zr wt. %	P wt. %
	21.11	14.31
TGA	Temperature range (°C)	% Weight loss
	40-180	1.48
	200-500	8.38
Surface area(BET method, )	36.75 m <sup>2</sup> /g	
Pore volume (ml/g)	0.62	
Total pore area (m <sup>2</sup> /g)	32.13	
NH <sub>3</sub> TPD	1.75 mmol/g	
X ray Diffraction	Crystalline, JCPDS Card no 33-1482	
FTIR	~3400cm <sup>-1</sup> (b) asymmetric and symmetric –OH stretches. ~1635cm <sup>-1</sup> (s) aquo (H–O–H) bending ~1035cm <sup>-1</sup> (m) P=O stretching. ~ 1400cm <sup>-1</sup> (m) δ(POH).	
SEM	Irregular morphology	

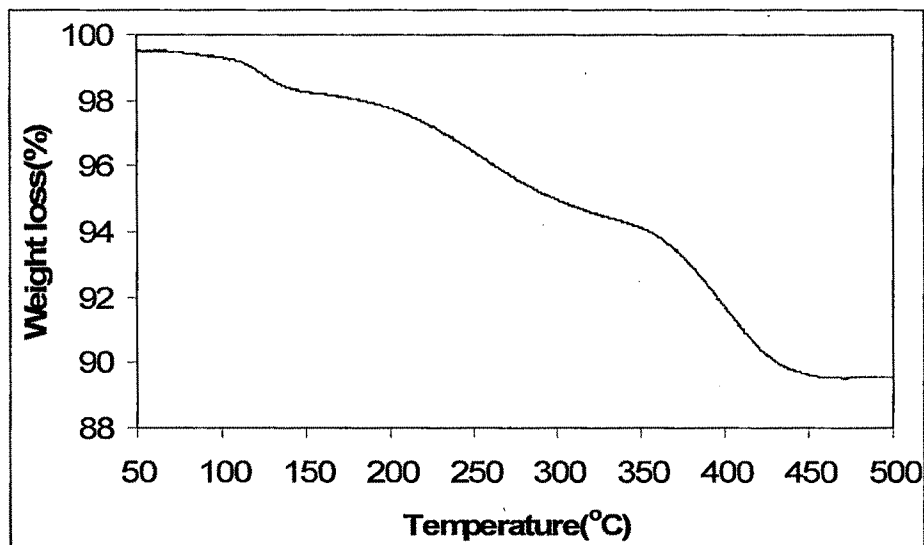


Figure 2.7a TGA of ZrPcry

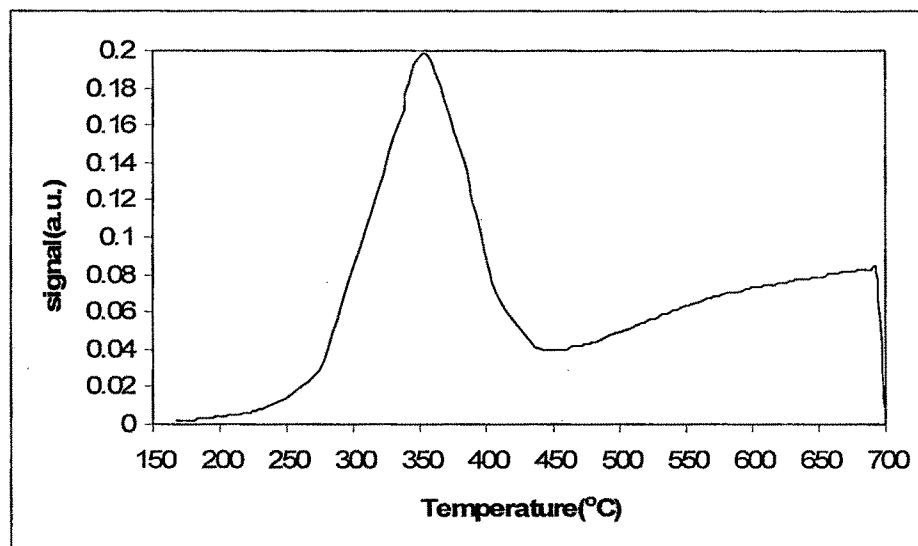


Figure 2.7b TPD pattern of ZrPcry

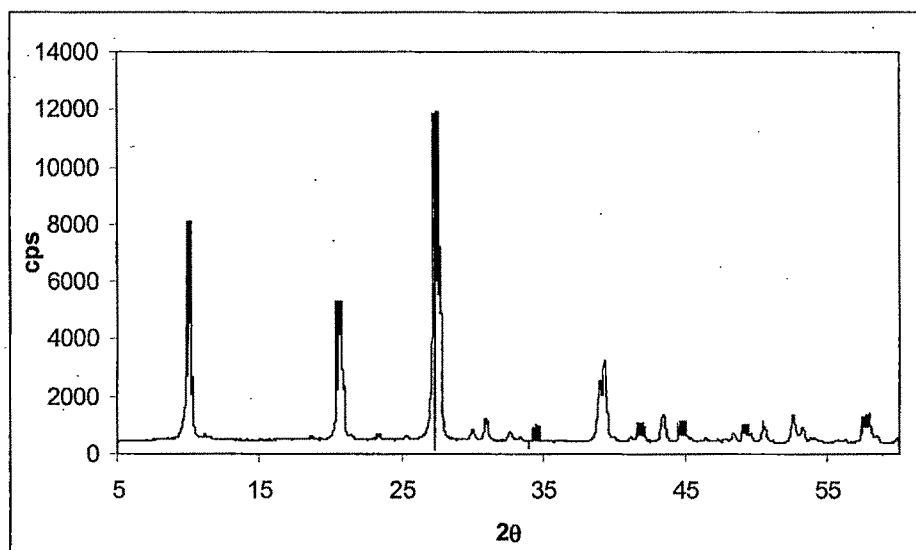


Figure 2.7c XRD of ZrPcry

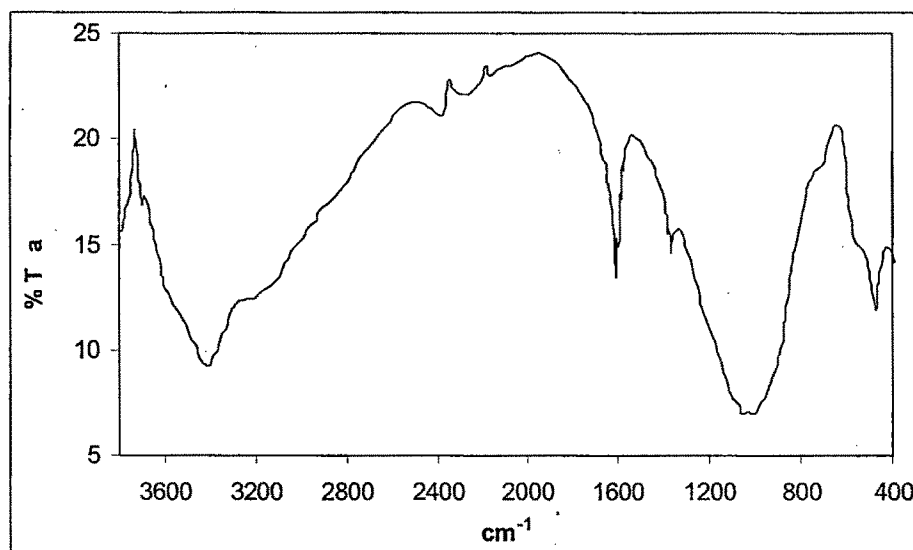
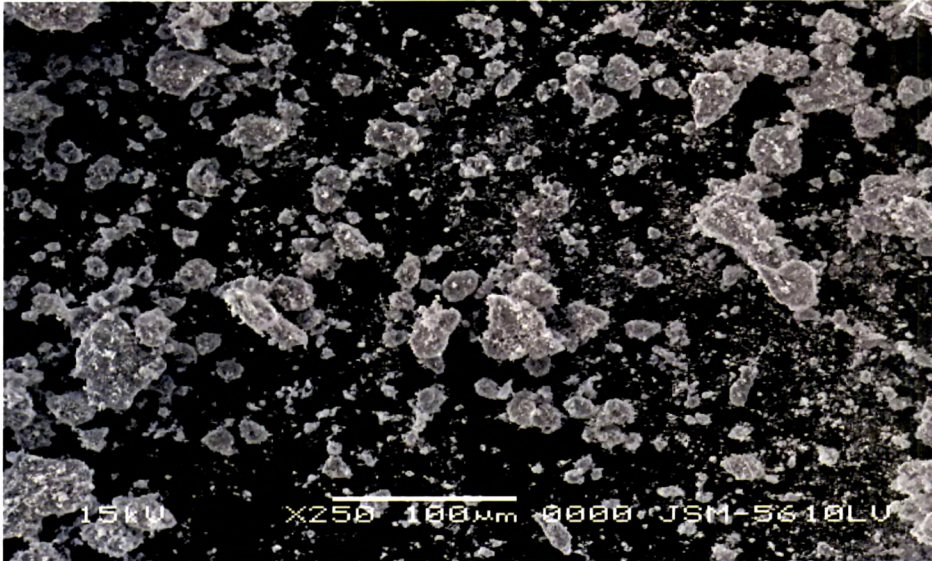


Figure 2.7d FTIR of ZrPcry



*Figure 2.7e SEM of ZrPcry*

**Table 2.8 Characterisation of TiPcry**

Characterization		
Chemical resistivity (maximum tolerable limits)	36N H <sub>2</sub> SO <sub>4</sub> , 16N HNO <sub>3</sub> , 10N HCl, 5N NaOH, 5N KOH, organic media (ethanol, propanol, butanol, benzyl alcohol, 2-ethyl 1-hexanol, anisole, veratrole, acetyl chloride, toluene, benzyl chloride, benzene, xylene acetone and acetic acid).	
Elemental analysis(ICP-AES)	Ti wt. %	P wt. %
	22.32	29.02
TGA Weight loss%,	Temperature range (°C)	% Weight loss
	40-180	4.01
	200-500	1.16
Surface area(BET method, )	28.00m <sup>2</sup> /g	
Mercury porosimetry	Pore volume (ml/g)	Total pore area (m <sup>2</sup> /g)
	0.75	36.56
NH <sub>3</sub> TPD	1.5 mmol/g	
X ray Diffraction	Crystalline, JCPDS Card no 44-0382	
FTIR	~3400cm <sup>-1</sup> (b) asymmetric and symmetric –OH stretches. ~1635cm <sup>-1</sup> (s) aquo (H–O–H) bending ~1035cm <sup>-1</sup> (m) P=O stretching. ~ 1400cm <sup>-1</sup> (m) δ(POH).	
SEM	Irregular morphology	

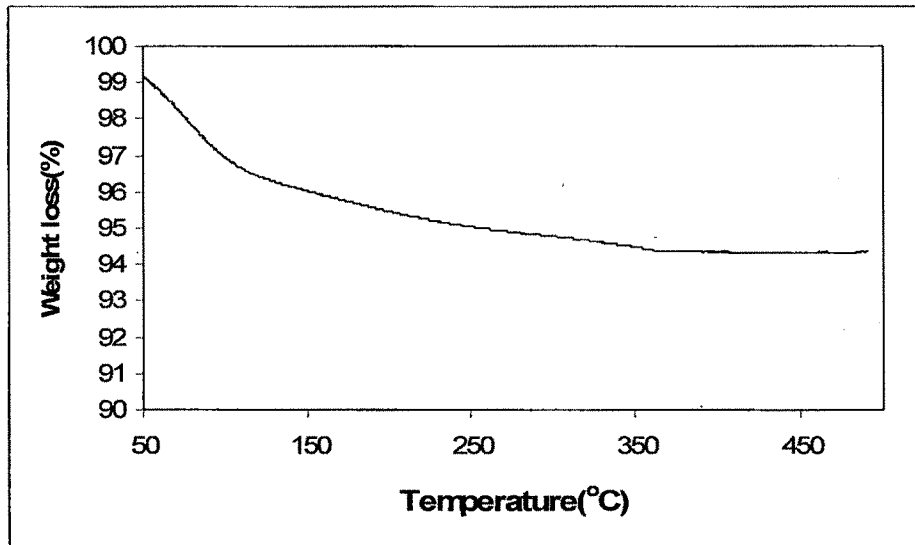


*Figure 2.8a TGA of TiPcry*

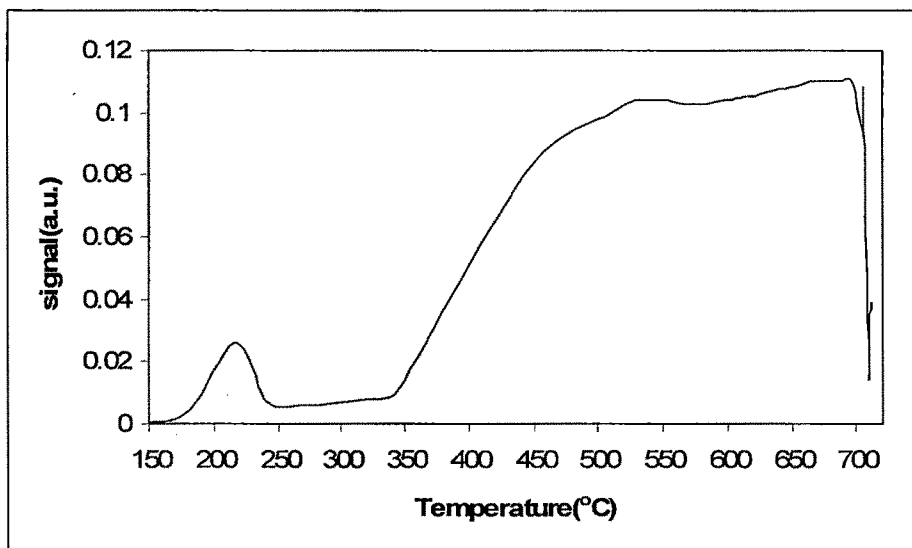


*Figure 2.8b TPD pattern of TiPcry*

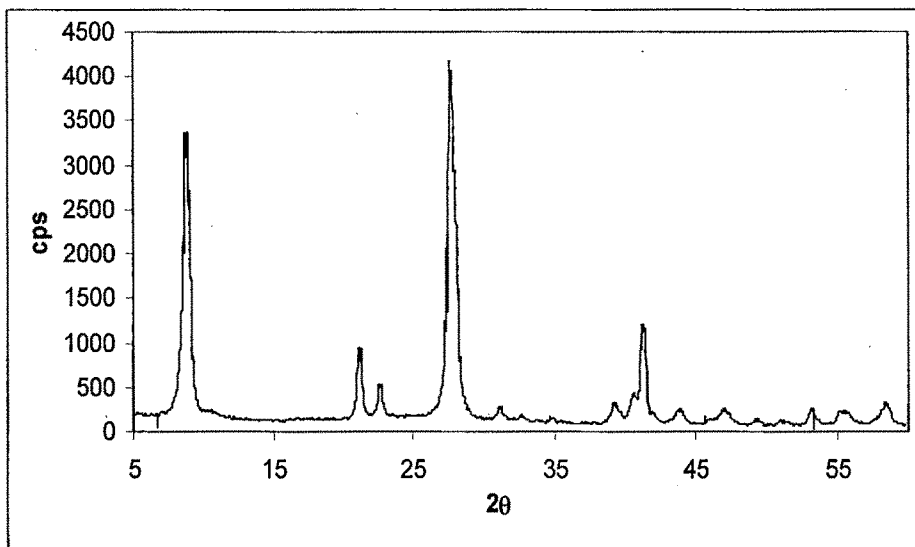


*Figure 2.8c XRD of TiPcry*

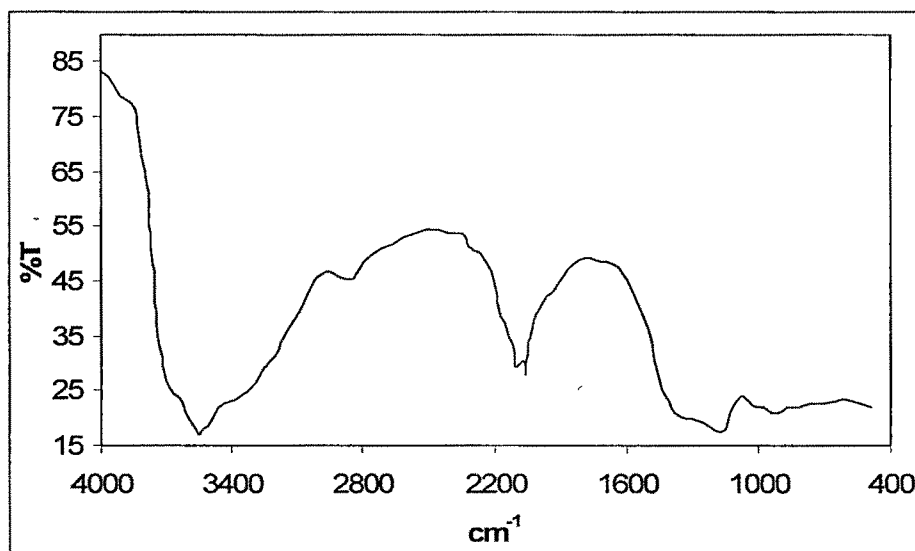


*Figure 2.8d FTIR of TiPcry*

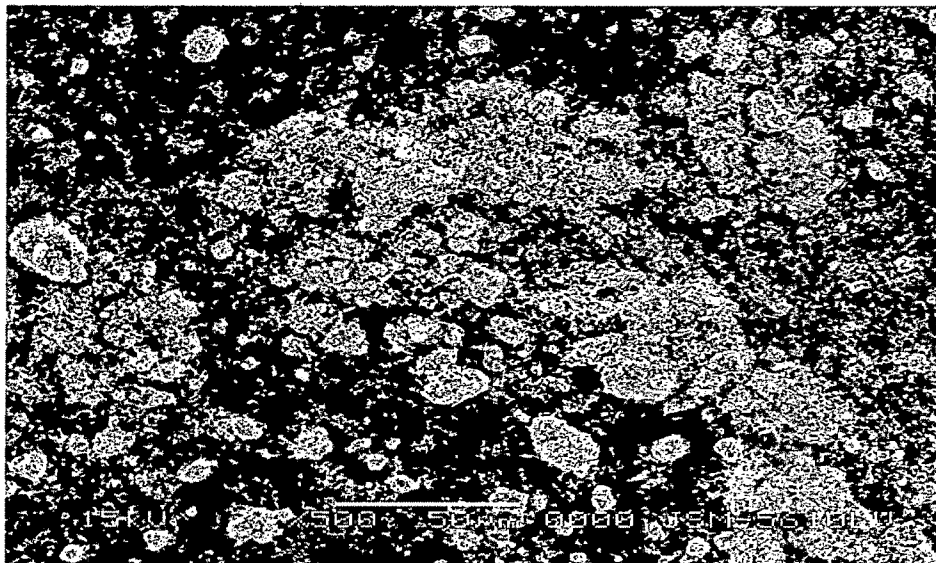


*Figure 2.8e SEM of TiPcry*

**Table 2.9 Characterisation of SnP<sub>cr</sub>**

Characterization		
Chemical resistivity (maximum tolerable limits)	36N H <sub>2</sub> SO <sub>4</sub> , 16N HNO <sub>3</sub> , 10N HCl, 5N NaOH, 5N KOH, organic media (ethanol, propanol, butanol, benzyl alcohol, 2-ethyl 1-hexanol, anisole, veratrole, acetyl chloride, toluene, benzyl chloride, benzene, xylene acetone and acetic acid).	
Elemental analysis(ICP-AES)	Sn wt. %	P wt. %
	28.16	14.6759
TGA	Temperature range (°C)	% Weight loss
	40-180	9.53
	200-500	2.07
Surface area(BET method )	25.00 m <sup>2</sup> /g	
Pore volume (ml/g)	0.24	
Total pore area (m <sup>2</sup> /g)	33.20	
NH <sub>3</sub> TPD	0.66 mmol/g	
X ray Diffraction	Crystalline, JCPDS Card no 39-0513	
FTIR	~3400cm <sup>-1</sup> (b) asymmetric and symmetric –OH stretches. ~1635cm <sup>-1</sup> (s)aquo (H–O–H) bending ~1035cm <sup>-1</sup> (m) P=O stretching. ~ 1400cm <sup>-1</sup> (m) δ(POH).	
SEM	Irregular morphology	

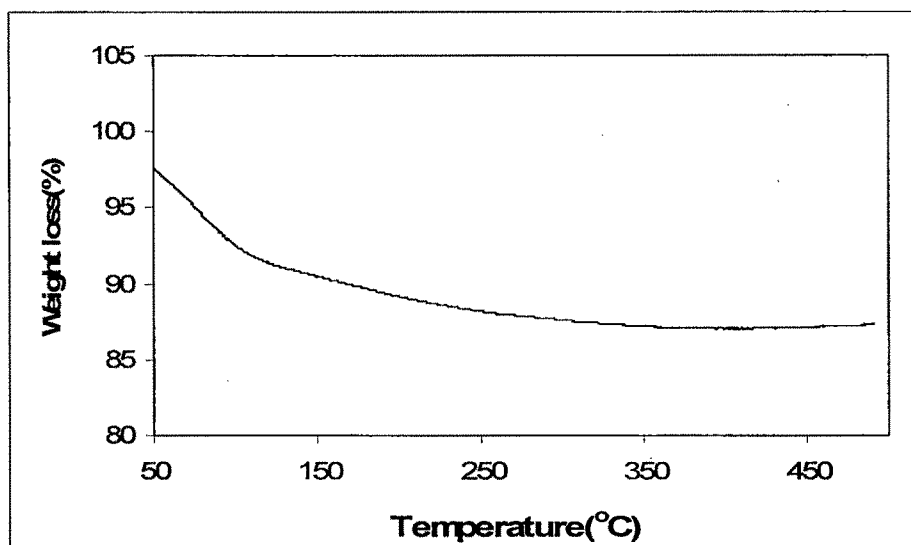


Figure 2.9a TGA of SnPcry

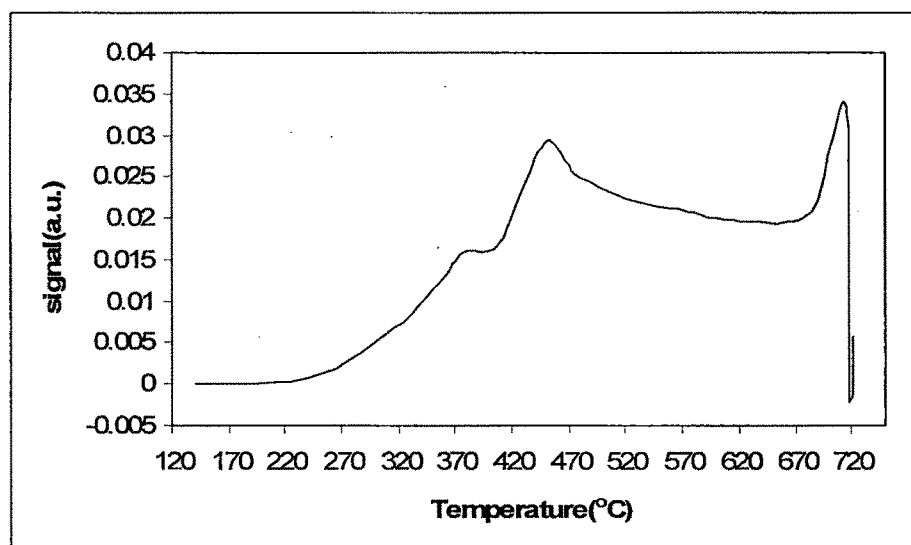
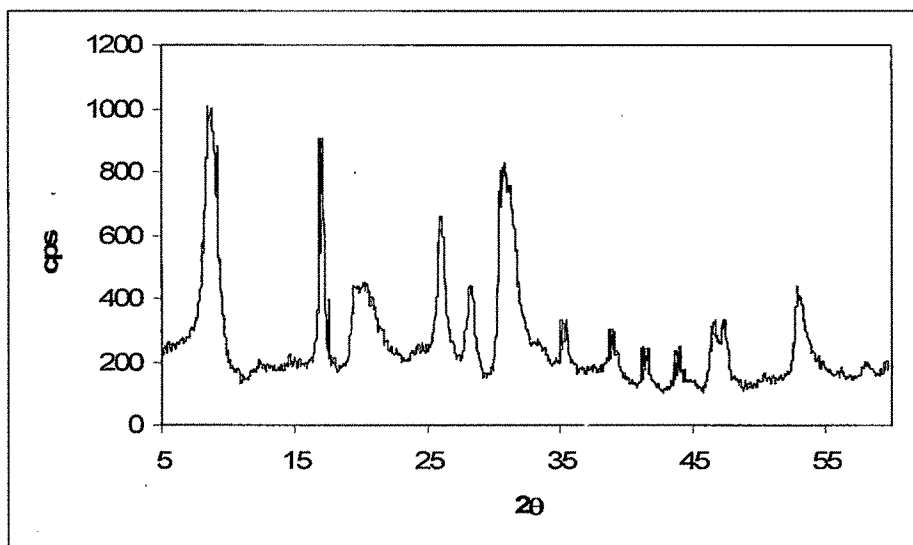
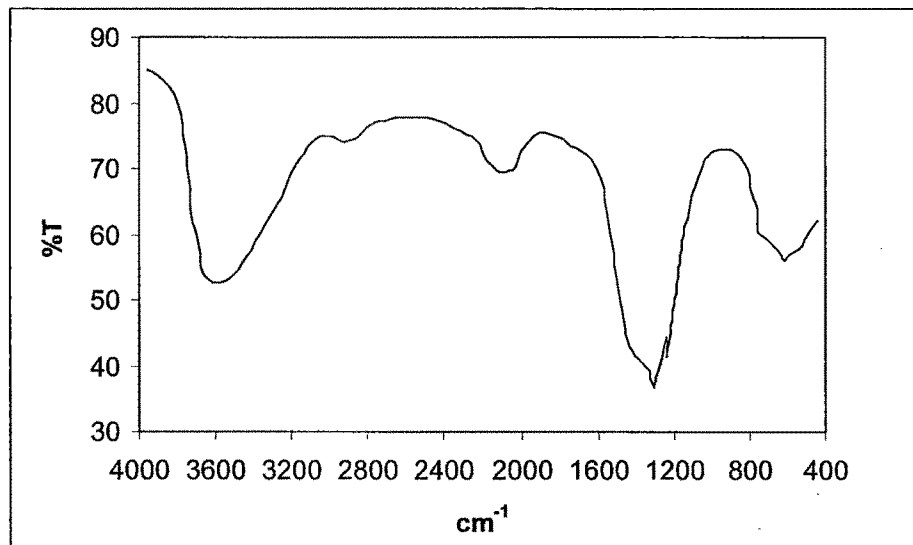


Figure 2.9b TPD pattern of SnPcry



*Figure 2.9c XRD of SnPcry*



*Figure 2.9d FTIR of SnPcry*



*Figure 2.9e SEM of SnPcry*

**REFERENCES**

- [1] Clearfield A and Thakur D S 1986 *App Catal* **26** 1.
- [2] Davis M E, Chem C Y, Burkett S L and Lobo F 1994 *Better Ceramics Through Chemistry VI* MRS Symposium Proceedings, Pittsburgh **Vol 346**
- [3] Kunin R 1971 *Elements of Ion Exchange* Robert E Krieger Publishing Company, New York.
- [4] Anderson J R and Pratt K C 1985 *Introduction to Characterization and Testing of Catalysts* Academic Press, Sydney
- [5] Haensel V and Haaensel H S 1989 *Characterization and Catalyst Development – An Interactive Approach* (Eds.) Bradly S A, Gattuso M J and Bertolacini R J. ACS Symposium Series 411
- [6] Nabi S A and Rao R K 1981 *J Ind Chem Soc* **11** 1030
- [7] Shannon R 1976 *Acta Crystallogr* **32A** 751
- [8] Young D M and Crowell A D 1962 *Physical Adsorption of Gases* Butterworths, London
- [9] Gregg S J and Sing K S W 1967 *Adsorption Surface Area and Porosity* Academic Press, London

**APPLICABILITY  
OF  
M(IV) PHOSPHATES  
AND  
M(IV) TUNGSTATES  
AS  
SOLID ACID CATALYSTS**